

COMPARATIVE ASSESSMENT OF PHYSICOCHEMICAL AND BACTERIOLOGICAL PARAMETERS IN WATER SOURCES NEAR MAJOR DUMPSITES AND CONTROL AREAS IN KARU-ABUJA AND PARTS OF NASARAWA STATE, NIGERIA

TYPE OF ARTICLE: ORIGINAL RESEARCH ARTICLE

ABSTRACT

This study evaluated the physicochemical and bacteriological parameters in water sources near major dumpsites and control areas in Karu-Abuja and Nasarawa State, to determine and compare extent of pollution using multivariate statistical analysis and indexing approach. Nine water samples from boreholes, hand-dug wells, and streams were analysed using AAS and standard methods. The concentration of Ca^{2+} , K^+ , Mg^{2+} , Cu^{2+} , Na^+ , Fe^{2+} , Zn^{2+} , F^- , SO_4^{2-} , CO_3^{2-} , pH, EC, COD, DO and BOD are within permissible limits, while parameters such as Pb^{2+} which varies from (0.44 to 0.488 mg/l), Co^{2+} (0.226 to 0.44 mg/l), Mn^{2+} (20.73 to 27.144 mg/l), Cr^{2+} (1.28 to 1.68 mg/l) and Cd^{2+} (0.09 to 0.092 mg/l) exceeded this limits. Results from Pearson correlation analysis ($p < 0.05$) showed positive correlations of r ranging from 0.5 to 1, indicating comparable sources of ions in the water systems. The Water Quality Index (WQI) for samples near dumpsites (177.72) indicated poorer quality compared to control areas (62.25). The study found that water samples from boreholes near control areas were suitable for domestic use with (WQI < 48), in contrast with samples from streams and hand-dug wells (WQI > 100). The water samples near dumpsites showed higher heavy metal pollution indices 188.53 compared to control sites 176.96. Bacterial analysis showed elevated coliform counts too numerous to be estimated (TNTC) in borehole samples near dumpsites, while streams had the lowest counts (9-16 cfu/ml) attributed to continuous flow. *E. coli*, *faecal strep*, and *Pseudomonas spp* were absent in most samples, except for a minor presence of (02 cfu/ml) *Pseudomonas spp* in a Keffi hand-dug well. The decreasing dominance for major cations and anions near dumpsites and control areas are: $\text{K}^+ > \text{Ca}^{2+} > \text{Cu}^{2+} > \text{Ni}^{2+} > \text{Na}^+ > \text{Mn}^{2+} > \text{Mg}^{2+} > \text{Zn}^{2+} > \text{Co}^{2+} > \text{Cr}^{2+} > \text{Pb}^{2+} > \text{Cd}^{2+}$; anions: $\text{F}^- > \text{SO}_4^{2-} > \text{Cl}^-$ and $\text{K}^+ > \text{Mn}^{2+} > \text{Ca}^{2+} > \text{Mg}^{2+} > \text{Cr}^{2+} > \text{Na}^+ > \text{Cu}^{2+} > \text{Co}^{2+} > \text{Zn}^{2+} > \text{Pb}^{2+} > \text{Cd}^{2+} > \text{Ni}^{2+}$; anions: $\text{Cl}^- > \text{SO}_4^{2-} > \text{F}^-$ respectively, attributed to anthropogenic and geogenic processes. Principal Component Analysis (PCA) accounted for over 92% of the total variance in water quality data. Hydrochemical plots identified mixed water types (Ca-Mg-HCO₃ and Ca-Mg-SO₄) with temporary hardness. The findings underscore the need for regular water quality monitoring and strategic siting of groundwater sources to mitigate contamination risks and protect public health.

Keywords: Heavy metal pollution index, water quality index, bacteria contamination, PCA

1. INTRODUCTION

The rapid population growth in Abuja, which increased from 378,671 in 1991 to 1,406,239 in 2006, has placed significant pressure on the city's infrastructure, exceeding the original master plan and the capacity of its water supply systems (NPCN, 2016; Jirikoet al. 2024). To address

the escalating water demand, residents in Karu-Abuja and parts of Nasarawa State, have turned to alternative water sources such as boreholes and hand-dug wells. However, these water sources are often located near open dumpsites, raising concerns about contamination from indiscriminate waste disposal. Open dumpsites generate leachate containing decomposing organic matter, heavy metals, and hazardous pollutants that can seep into groundwater aquifers, potentially compromising water quality (Emenike *et al.* 2024; Singh *et al.* 2024). Contaminants such as heavy metals, including cadmium (Cd), arsenic (As), and lead (Pb), pose serious health risks due to their bioaccumulation in body tissues, despite their trace presence being essential for certain physiological functions (Raimi *et al.* 2022; Ukahet *et al.* 2019; Egbueri and Unigwe, 2020). These risks necessitate comprehensive evaluations of water quality to safeguard public health and inform effective water management policies. Previous studies have underscored the impact of pollution on water quality. For example, some researchers investigated the dynamics in physicochemical and microbiological properties of simulated leachate from dumpsite soil in Ikhueni, Edo State, Nigeria, using standard Microbiological testing techniques (Obute *et al.* 2024). They collected samples from a non-sanitary open dumpsite in the study area, and leachate by filtering 150 g of waste-impacted soil mixed with sterile distilled water (1000 mL). Results indicated high densities of microbial contamination with total heterotrophic bacteria (1.5 ± 0.5 to $6.9 \pm 1.0 \times 10^4$ CFU mL⁻¹) and coliform (2.7 ± 0.8 to $7.8 \pm 1.0 \times 10^3$ CFU mL⁻¹) counts. Physicochemical analyses revealed significant ($p < 0.05$) variations in parameters such as EC with values ranging from 9183.3 – 9758.7 μscm^{-1} , TDS with values ranging from 7004.0 – 8210.3 ppm, with changes in pH ranging from 6.48-7.62, biochemical oxygen demand (BOD) with values ranging from 561.7 – 651.3 mgL⁻¹, and chemical oxygen demand (COD) with values ranging from 1981.7-2058.7 mgL⁻¹. The pH dropped from 7.62 to 6.48, and the levels of BOD and COD indicated a decreasing trend that was strongly and positively correlated (“r” ranging from 0.949 to 0.968) with bacterial counts, indicating organic molecule degradation. Ocheoibo and Atuanya (2024) evaluated the microbial load and physicochemical characteristics of soils in electronic waste dumpsites of Oluku and Osasogie in Benin, Edo State and Alaba in Lagos State, Nigeria, using appropriate standard procedures. The mean bacterial counts on Nutrient agar (NA) ranged between 9.00 ± 2.646 cfu/g and 5.33 ± 1.202 cfu/g. The highest fungal count recorded in the control site (10.67 ± 1.764 cfu/g) and the lowest count (3.33 ± 0.882 cfu/g) was recorded at Alaba. Adeleke and Faraday (2024) evaluated the microbial contamination and quality indicators of

groundwater in the coastal environment of Ondo State, Nigeria. They collected nine underground water samples from the study area and assayed using conventional microbiological techniques coupled with standard physical and chemical analytical procedures. Results revealed that all the samples had total viable bacterial counts, fungal counts and coliform counts which ranged from 61.25 to 85.32 CFU/100 mL, 10.00 to 35.32 SFU/100 mL and 6 – 24 MPN/100 mL respectively, which were higher than the set WHO limit. Results also revealed that the samples from Irele and Ese- OdoLGA had acidic pH in the range of 4.20 -5.21 considered to be below the WHO permissible limit whereas only one of three samples from Ilaje LGA had acidic pH of 5.23. The concentrations of the heavy metals varied among the samples with manganese (0.183-0.311) mg/L exceeding the 0.08 mg/L prescribed by the WHO. Arufet *al.*(2024) analysed ten water samples from eight distinct areas within Kano State, Nigeria. Results revealed that PH levels ranged from 6.50 to 7.20, falling within the permissible range recommended by the WHO. The highest turbidity was 51.66 NTU. Hardness ranged from 158.6 to 297.7 mg/L, falling within the limit. Alkalinity levels surpassed the standard in most areas, while TDS fell below the standard. Cadmium concentrations ranged from 0.04 mg/L to 0.162 mg/L, with both values exceeding the WHO limit. Nickel levels ranged from 0.369 mg/L to 1.288 mg/L, surpassing the WHO recommendation of 0.2 mg/L. Lead concentrations reached alarming levels, exceeding the recommended value of 1.00 mg/L, with Municipal and Fagge recording concentrations of 3.7882 mg/L and 3.5627 mg/L respectively. Chromium concentrations varied from 0.82 mg/L to 4.4 mg/L, all surpassing the WHO limit. The study suggested that gastrointestinal illnesses, chronic kidney disease and cardiovascular diseases is associated with poor water quality. Abdu-Raheem *et al.*(2024) applied hydrogeochemistry and bacteriological analysis to evaluate portability and status of shallow wells' water in Iworoko-Ekiti, Southwest Nigerian for domestic and irrigational uses. Water Quality Index (*WQI*) evaluation revealed that only 26.7% of the water samples fell in the good to excellent water categories while the rest (73.3%) were in unfit to poor water classes. The studies further revealed that all chemical values were within standard for drinking water except nitrate in which 93% of the water samples had concentrations above the approved 50-mg/l standard for drinking water.

2. LOCATION AND GEOLOGY

The study areas are situated between latitude 8°50'16.7994"N and 8°50'38.4822"N and longitudes 7°53'15.36"E and 7°53'2.5002"E in parts of Karu-Abuja, Goshen City and Keffi in Nasarawa State.

The sampling points include: A Stream under Karu-Abuja Bridge dumpsite (A); A borehole near Junior Sec. School along Jikwoyi-Karachi road, Karu-Abuja dumpsite (control) (B); A Stream adjacent the Karu-Abuja dumpsite along Jikwoyi-Karachi road (C); A Hand-Dug Well near Goshen control (D); Hand-Dug Well near Keffi Control (E); A borehole in Keffi control (F); A Hand-Dug Well near Goshen dumpsite in Aso-Kadepe area, Karu LGA, Nasarawa State(G); a borehole near Tipper Garage dumpsite Karu-Abuja (H); and a borehole near the Baptist Church dumpsite, Panteka area in Keffi (I).The study area is underlain by basement complex rocks of Nigeria, including migmatite gneisses, schist belts, Older Granites suite, charnockites, syenites, minor gabbroic, dioritic rocks and undeformed acid and basic dykes. (Dada, 2006). The general structures include joints, foliations, and faults (Dada, 2006).The region is characterized by highlands and lowlands with elevations below 260 meters, particularly around the S-E, near the River Uke flow path. The highest relief point, located around S-W, reaches heights of 410 m (asl) and is an intrusive outcrop. The study areas are influenced by two major climatic conditions: the rainy season from April to October and the dry season from February to early-mid April. The annual rainfall average is 145.66 mm (Bashir, 2018). The drainage pattern of the area is dendritic, indicating resistance to erosion by the underlying rock units.

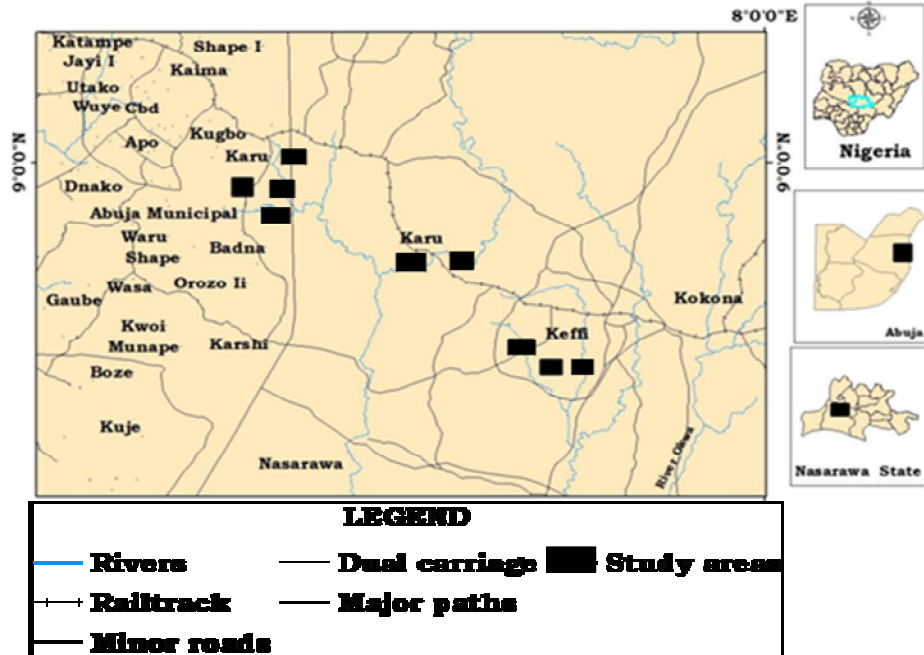


Figure 1: Map of the study areas showing the sampling points (after NASRDA, 2018).

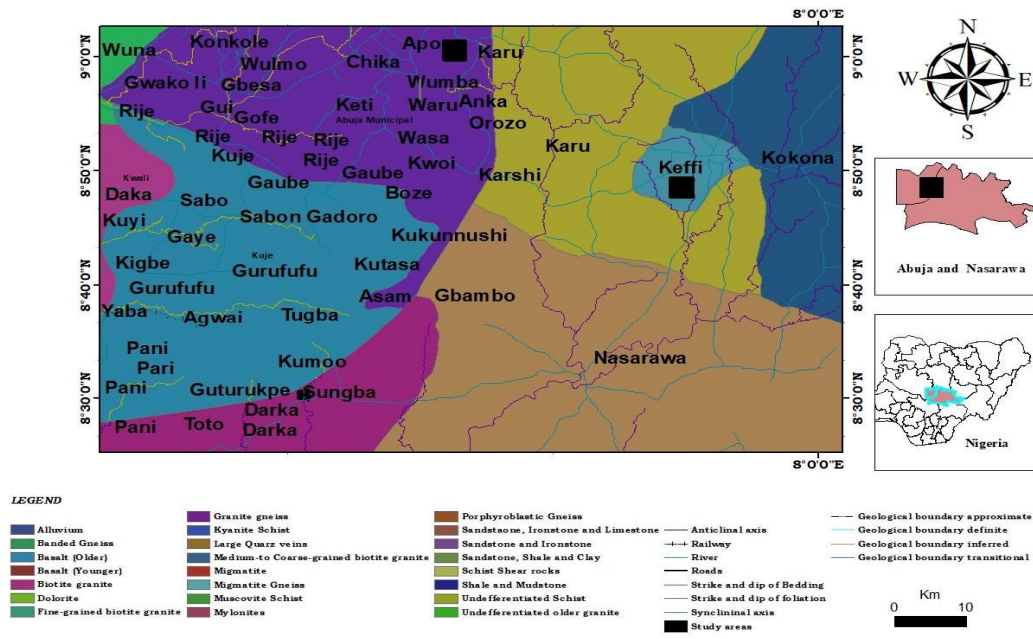


Figure 2: Geological map of the study areas (after NGSA, 2011)

3. MATERIAL AND METHODS

3.1 Water Sample Collection and Processing

Nine water samples were collected from various sources, including boreholes, hand-dug wells, and streams. Five samples were taken near dumpsites, while four were collected from control areas located approximately 700 meters away from the dumpsites. Pre-rinsed polyethylene bottles were thoroughly scrubbed three times with the water sample before collecting representative samples. Prior to sampling, the bottles were sanitized with a solution of 20% nitric acid (HNO_3), thoroughly rinsed with distilled water and air-dried. Each collected sample was labelled appropriately and transported to Sheda Laboratory in Kwali-Abuja in an insulated container filled with ice. Upon arrival, the samples were stored in a freezer at 4 °C to maintain their integrity until analysis. The analysed parameters are compared to guidelines from the World Health Organization (WHO, 2017, 2011, 2008, and 2004), Standard Organisation of Nigeria (SON, 2015), and Nigeria Standard for Drinking Water Quality (NSDWQ, 2007). Violation rates of water quality attributes are calculated accordingly. The Kaiser-Meyer-Olkin (KMO) test and Cronbach's alpha coefficient were used to assess sample adequacy and reliability of the data. Tools such as GRAPHER, SURFER, and XLSTAT are used to construct Piper and Durov plots for characterizing water composition (Piper, 1944; Durov, 1948). Laboratory results are subjected to multivariate statistical analysis, including indexing, Principal Component Analysis (PCA), and hydrochemical facies analysis. The Pearson's pairwise correlation at a 0.05 significance level is used to evaluate relationships between parameters.

3.2 Experimental Procedures

To ensure accurate characterization of the physicochemical and microbiological quality of water samples in the study area, we followed a systematic approach from field measurements to the various analyses explained below.

3.2.1 Field Measurements

Temperature is measured on-site using a mercury-in-glass portable thermometer. Turbidity readings are obtained using the nephelometric method with a HACH 2100AN turbidimeter (APHA, 1998), while pH (hydrogen ion concentration) level is determined with HANNA pH meter (Model HI 28129). The Electrical Conductivity (EC) and Total Dissolved Solids (TDS) are measured following standard APHA (2005) procedures.

3.2.2 Chemical Analysis

The following minor and trace elements were analysed, namely: Calcium (Ca^{2+}), Lead (Pb^{2+}), Cobalt (Co^{2+}), Nickel (Ni^{2+}), Potassium (K^+), Magnesium (Mg^{2+}), Copper (Cu^{2+}), Manganese (Mn^{2+}), Sodium (Na^+), Chromium (Cr^{2+}), Iron (Fe^{2+}), Zinc (Zn^{2+}), Cadmium (Cd^{2+}) using atomic absorption spectrophotometer (AAS) with air-acetylene gas mixture as oxidant. The samples were aspirated after calibrating the equipment with relevant standard solutions for each element. The results were recorded in mg/L. Major ions like Chloride (Cl^-), carbonate (CO_3^{2-}), sulfate (SO_4^{2-}), calcium (Ca^{2+}), magnesium (Mg^{2+}), sodium (Na^+), and potassium (K^+) are analysed using standard APHA methods (2005). Biochemical Parameters such as Biological Oxygen Demand (BOD), Dissolved Oxygen (DO), and Chemical Oxygen Demand (COD) are measured with a Hanna HI98193 waterproof portable meter and probe. Iron (Fe^{2+}) and manganese (Mn) are quantified using a Perkin Elmer PinAAcle 500 instrument. While Fluoride ion (F^-) is measured with a potentiometric ion-selective probe (Hanna HI5316).

3.2.3 Bacteria Contamination Analyses

For bacteriological analysis, water samples were collected in duplicate inside 250-mL sterile glass bottles. The samples inside sterile bottles were tightly capped, maintained in vertical position, kept in cooler filled with ice blocks before onward transmission to the laboratory. The water samples are also kept at 4°C before proper analysis. The glass wares used were washed and sterilized in a hot-air oven at 160°C for 1 hour. The inoculating loop and needles were sterilized by flaming to red hot and allowed to cool (APHA, 1998). The work bench was disinfected with cotton wool soaked in 70% ethanol before and after analysis. The 9 samples collected in disposable bottles were sterilized and transported to the laboratory for coliform detection and isolation of microorganisms within 24 - 48 hours of collection. Multiple tubes techniques were used for detection of coliform in the water sample. Lactose broth was prepared to industrial standard specification with phenol red as indicator. The lactose broth (10 ml) was dispensed into test tubes as single strength while double concentration of the lactose was used as double strength for the lactose fermentation. The media used were Plate Count Agar, Nutrient agar (HiMedia Laboratories Limited, India), Eosin Methylene Blue agar (HiMedia Laboratories Limited, India) and Triple Sugar Iron (TSI) agar (Lab M Limited, United Kingdom). All the media were prepared according to the manufacturer's instructions and sterilized in the autoclave at 121°C for 15 minutes. The water sample (1 ml) was inoculated into plate count medium using

pour plating technique and then incubated at 37⁰C for 24 hours. This method quantified colony-forming units per 100 mL (cfu/100 mL) of water (APHA, 1998).

3.5 Photographs from the field



Plate 1: Water sources for samples collected near the dumpsites

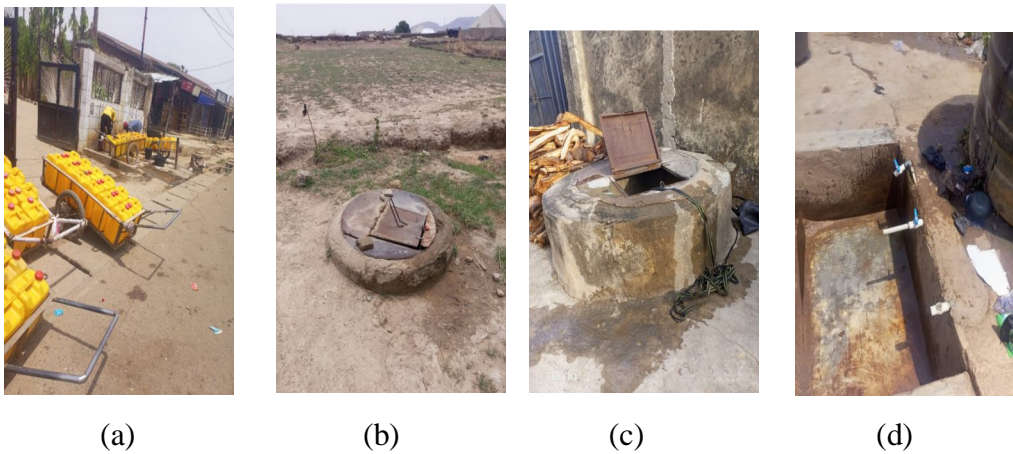


Plate 2: Water sources for samples collected around the control sites

4. RESULT

4.1 Analysed Water Parameters

The results of analysed parameters for water samples collected near the dumpsites and control areas in Karu-Abuja, Goshen areas and Keffi in Nasarawa State, showing the minimum, maximum, standard deviation, mean values and acceptable concentration limits as prescribed by standard organisations are presented in Tables 1 and 2:

Table 1: The statistics of the analysed parameters of water samples collected around the dumpsites

Parameters	Minimum	Maximum	Standard Deviation	Mean	Standard	Source/Year
Major Cations						
Ca ²⁺ (mg/L)	8.690	51.550	16.796	22.510	75.0	WHO, 2017
Pb ²⁺ (mg/L)	0.040	1.070	0.407	0.440	0.01	SON, 2015
Co ²⁺ (mg/L)	0.000	0.650	0.271	0.256	0.005	WHO, 2008
Ni ²⁺ (mg/L)	0.000	0.000	0.000	0.000	0.02	NSDWQ, 2007
K ⁺ (mg/L)	1.740	16.860	6.081	10.988	100.0	WHO, 2011
Mg ²⁺ (mg/L)	1.170	41.310	15.185	17.986	50.0	WHO, 2011
Cu ²⁺ (mg/L)	0.000	1.060	0.436	0.704	1.0	NSDWQ, 2007
Mn ²⁺ (mg/L)	14.410	37.240	9.623	27.144	0.2	NSDWQ, 2007
Na ⁺ (mg/L)	0.610	1.010	0.160	0.890	50.0	WHO, 2011
Cr ²⁺ (mg/L)	0.170	1.990	0.672	1.284	0.05	WHO, 2011
Fe ²⁺ (mg/L)	0.000	0.210	0.093	0.096	0.3	WHO, 2011
Zn ²⁺ (mg/L)	0.370	0.430	0.025	0.400	3.0	NSDWQ, 2007
Cd ²⁺ (mg/L)	0.050	0.130	0.032	0.092	0.003	NSDWQ, 2007
Major Anions						
F ⁻ (mg/L)	0.850	2.520	0.692	1.650	1.0	WHO, 2011
SO ₄ ²⁻ (mg/L)	1.000	20.000	8.289	11.800	200.0	WHO, 2011
Cl ⁻ (mg/L)	47.920	730.740	282.028	257.796	200.0	WHO, 2011
CO ₃ ²⁻ (mg/L)	0.000	0.000	0.000	0.000	-	-
pH	6.300	7.600	0.522	7.006	6.50-8.50	WHO, 2011
EC (µS/cm)	204.800	849.800	278.604	521.120	750.0	WHO, 2011
COD (mg/L)	12.800	29.580	6.310	18.968	80.0	WHO, 2004
Turb (NTU)	0.340	15.600	7.142	7.038	5.0	WHO, 2011
TDS (µs/cm)	100.400	422.500	138.439	256.460	500.0	WHO, 2011

DO (mg/L)	2.800	6.200	1.332	4.040	5.0	NSDWQ, 2007
BOD (mg/L)	1.900	5.000	1.114	3.320	5.0	NSDWQ, 2007
Temp. °C	31.000	34.000	1.182	32.780	30.0	NSDWQ, 2007

Source: Laboratory analysis

Note: CFU/ML- Colony Forming Unit per milliliter

Table 2: The statistics of the analysed parameters of water samples collected around the control sites

Parameters	Minimum	Maximum	Standard Deviation	Mean	Standard	Source/Year
Major Cations						
Ca ²⁺ (mg/L)	2.930	19.570	7.455	11.908	75.0	WHO, 2017
Pb ²⁺ (mg/L)	0.240	1.010	0.357	0.488	0.01	SON, 2015
Co ²⁺ (mg/L)	0.100	0.630	0.236	0.440	0.005	WHO, 2008
Ni ²⁺ (mg/L)	0.000	0.200	0.100	0.050	0.02	NSDWQ, 2007
K ⁺ (mg/L)	1.510	42.700	19.266	14.045	100.0	WHO, 2011
Mg ²⁺ (mg/L)	0.580	17.650	7.790	9.218	50.0	WHO, 2011
Cu ²⁺ (mg/L)	0.430	1.140	0.372	0.800	1.0	NSDWQ, 2007
Mn ²⁺ (mg/L)	9.860	32.730	9.632	20.730	0.2	NSDWQ, 2007
Na ⁺ (mg/L)	0.370	2.480	0.947	1.085	50.0	WHO, 2011
Cr ²⁺ (mg/L)	1.170	2.410	0.578	1.683	0.05	WHO, 2011
Fe ²⁺ (mg/L)	0.000	0.000	0.000	0.000	0.3	WHO, 2011
Zn ²⁺ (mg/L)	0.390	0.440	0.021	0.415	3.0	NSDWQ, 2007
Cd ²⁺ (mg/L)	0.070	0.130	0.028	0.090	0.003	NSDWQ, 2007
Major Anions						
F ⁻ (mg/L)	0.020	1.250	0.522	0.518	1.0	WHO, 2011
SO ₄ ²⁻ (mg/L)	4.000	65.000	28.408	27.500	200.0	WHO, 2011
Cl ⁻ (mg/L)	39.930	258.550	96.156	135.015	200.0	WHO, 2011
CO ₃ ²⁻ (mg/L)	0.000	0.000	0.000	0.000	-	-
pH	6.540	7.010	0.199	6.820	6.50-8.50	WHO, 2011
EC (µs/cm)	127.40	535.700	183.313	352.925	750.0	WHO, 2011
COD (mg/L)	8.760	25.450	7.487	18.955	80.0	WHO, 2004
Turb (NTU)	0.210	15.200	7.038	5.060	5.0	WHO, 2011
TDS (mg/L)	62.670	263.000	90.034	173.343	500.0	WHO, 2011
DO (mg/L)	0.400	5.800	2.417	3.800	5.0	NSDWQ, 2007
BOD (mg/L)	0.010	4.900	2.175	3.203	5.0	NSDWQ, 2007
Temp. °C	31.300	34.300	1.484	32.075	30.0	NSDWQ, 2007

Source: Laboratory analysis

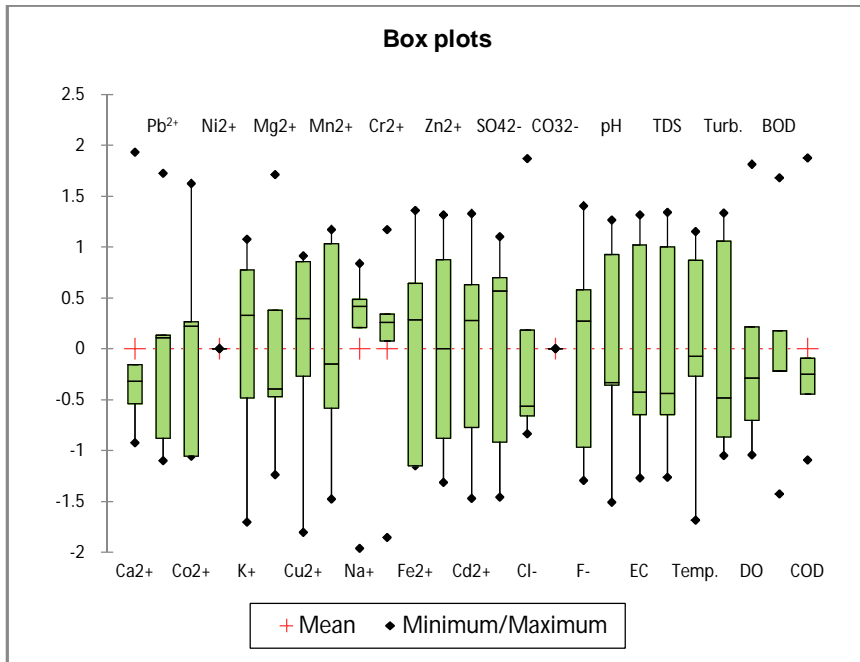


Figure 3: Box plot for water samples collected near dumpsites

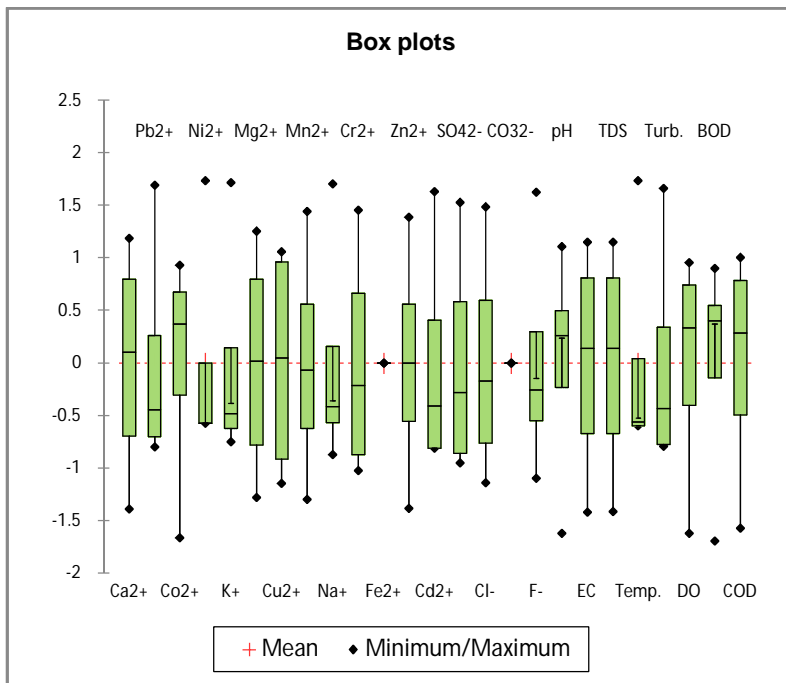


Figure 4: Box plot for Water samples collected near the control areas

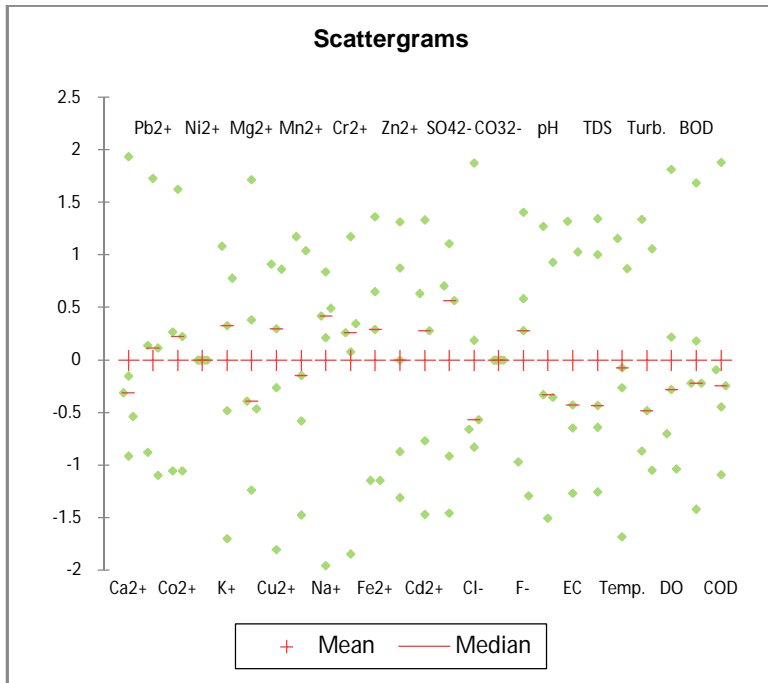


Figure 5: Scattergrams for Water samples collected near the dumpsites

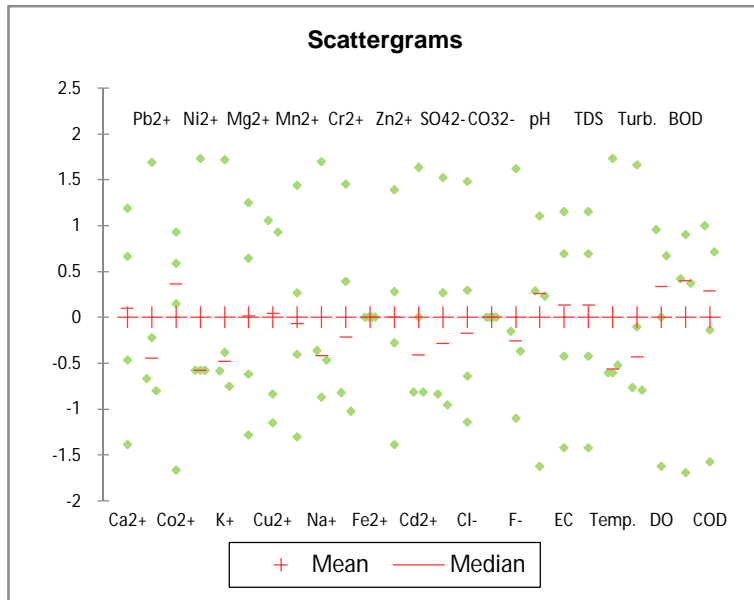
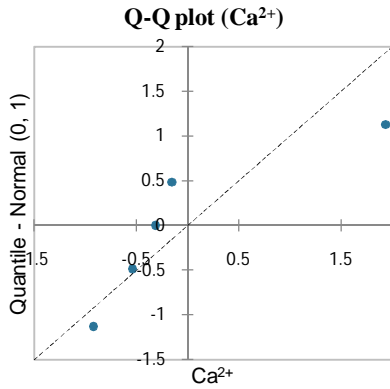
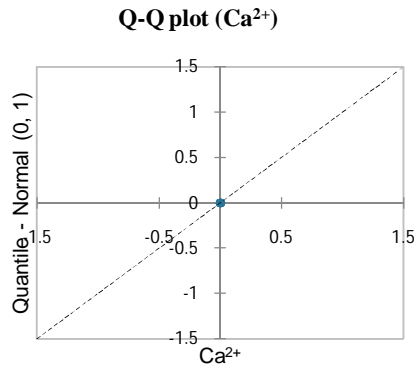


Figure 6: Scattergrams for Water samples collected near the control areas

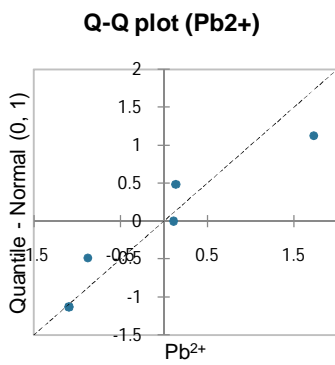


i)

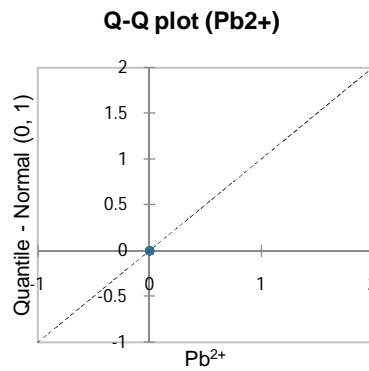


ii)

Figure 7: QQ-Plot for Ca ions in water samples collected near the dumpsites and control areas

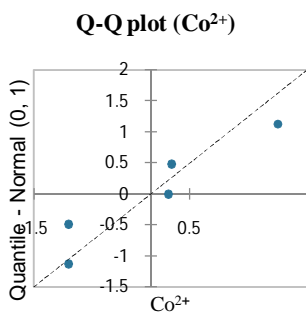


ii)

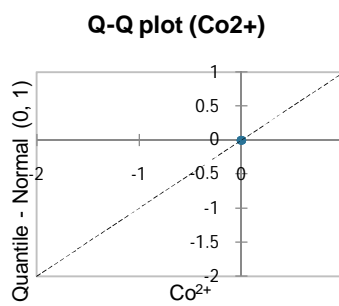


iv)

Figure 8: QQ-Plot for Pb ions in water samples collected near the dumpsites and control areas



vi)



v)

Figure 9: QQ-Plot for Co ions in water samples collected near the dumpsites and control areas

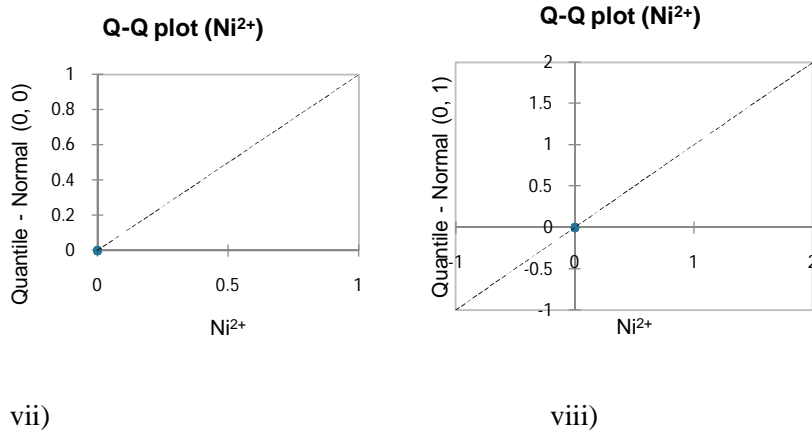


Figure 10: QQ-Plot for Ni ions in water samples collected near the dumpsites and control areas

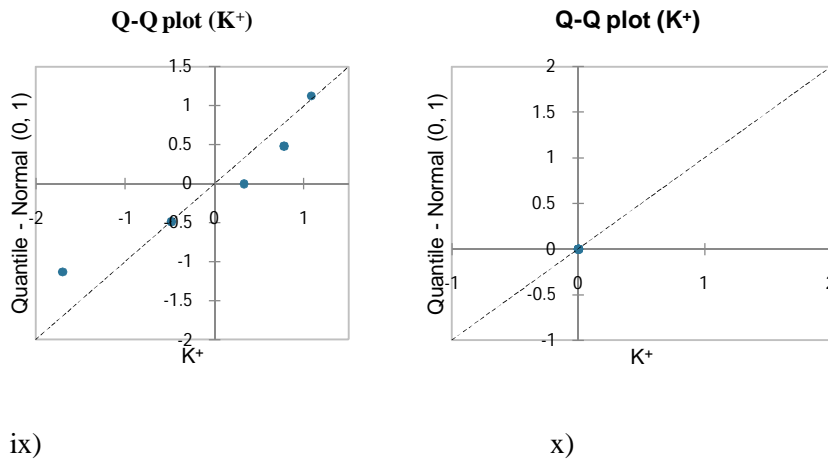
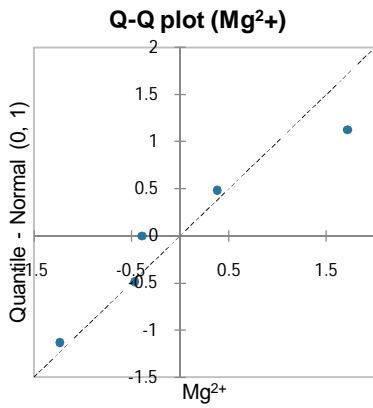
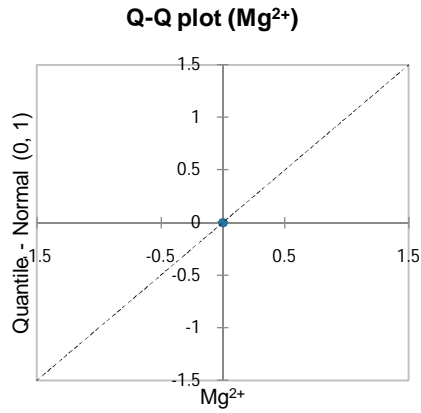


Figure 11: QQ-Plot for K ions in water samples collected near the dumpsites and control areas

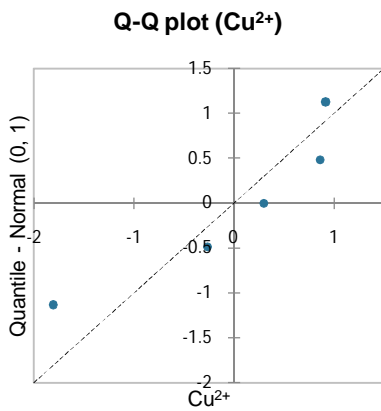


xi)

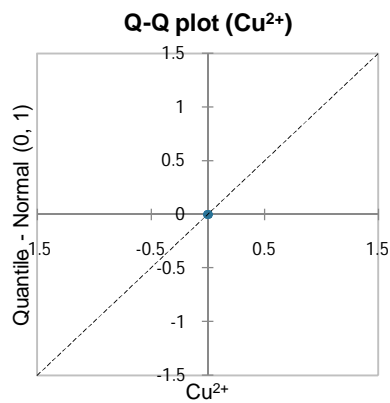


xii)

Figure 12: QQ-Plot for Mg ions in water samples collected near the dumpsites and control areas

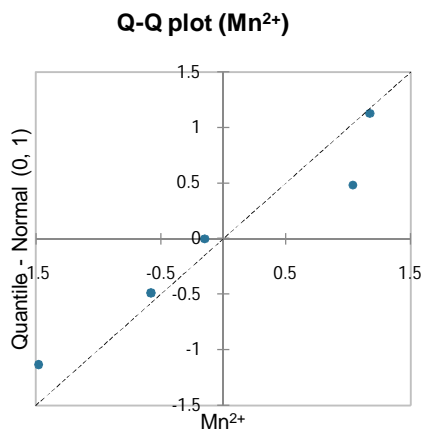


xiii)

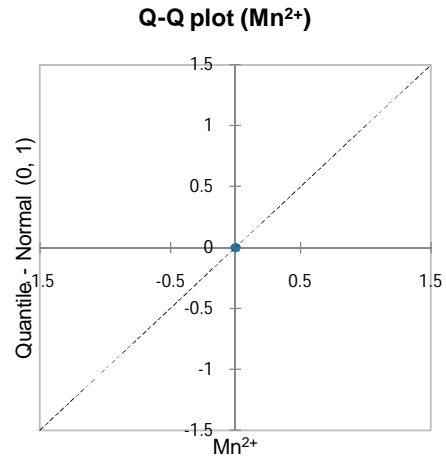


xiv)

Figure 13: QQ-Plot for Cu ions in water samples collected near the dumpsites and control areas

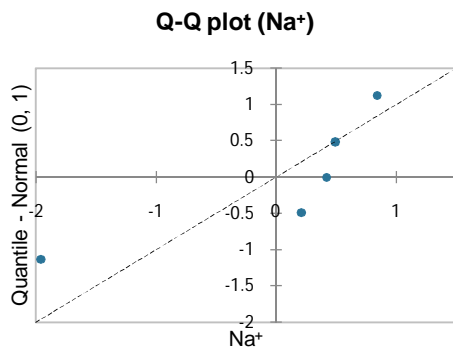


xv)

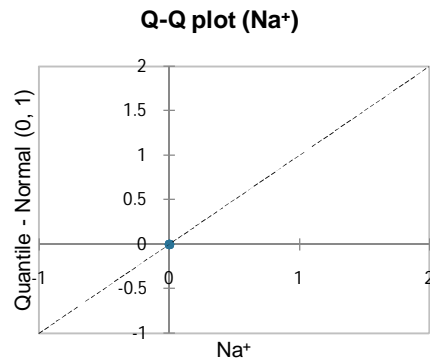


xvi)

Figure 14: QQ-Plot for Mn ions in water samples collected near the dumpsites and control areas

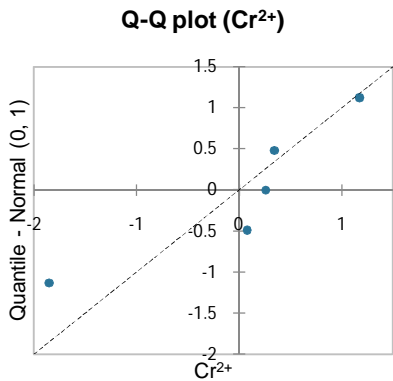


xvii)

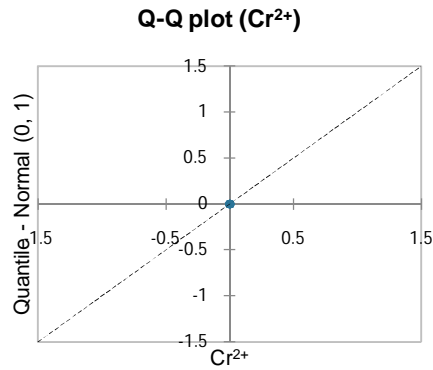


xviii)

Figure 15: QQ-Plot for Na ions in water samples collected near the dumpsites and control areas

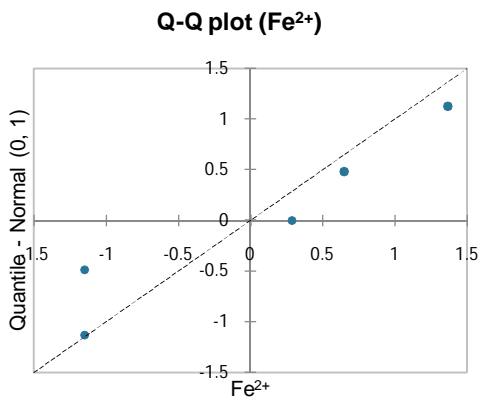


xix)

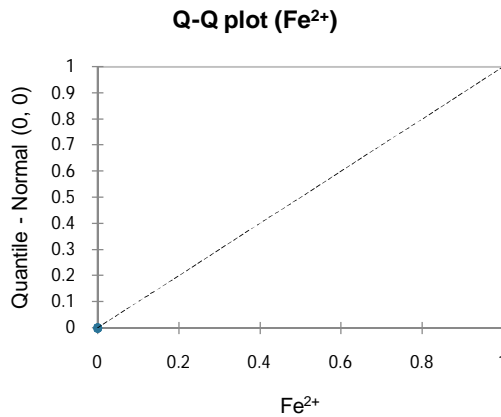


xx)

Figure 16: QQ-Plot for Cr ions in water samples collected near the dumpsites and control areas

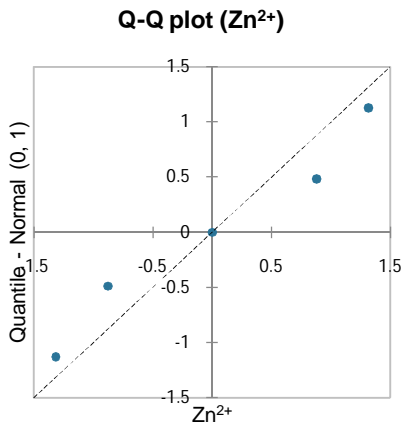


xxi)

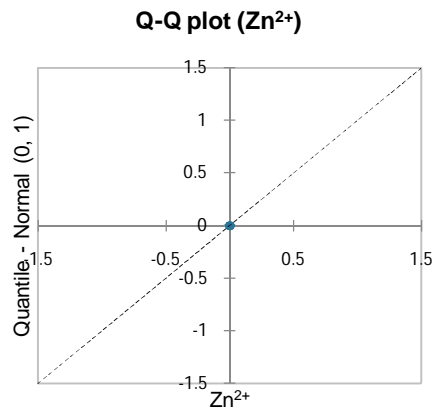


xxii)

Figure 17: QQ-Plot for Fe in water samples collected near the dumpsites and control areas

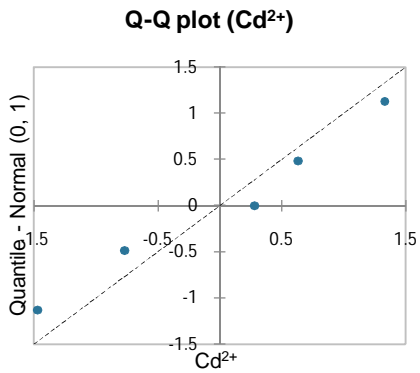


xxiii)

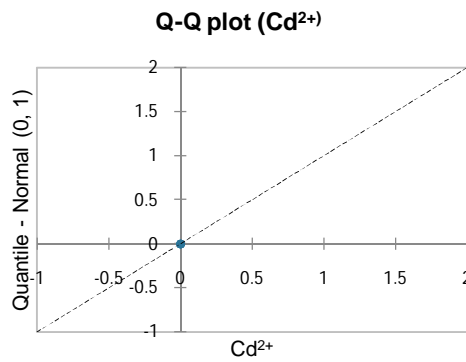


xxiv)

Figure 18: QQ-Plot for Zn ions in water samples collected near the dumpsites and control areas

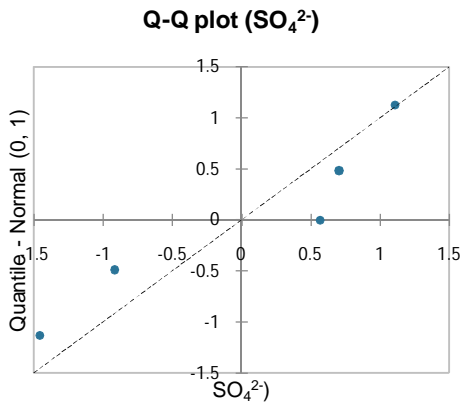


xxv)

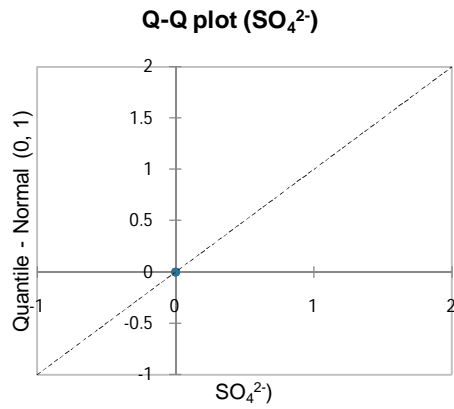


xxvi)

Figure 19: QQ-Plot for Cd ions in water samples collected near the dumpsites and control areas

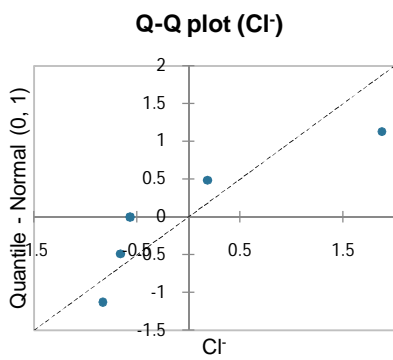


xxvii)

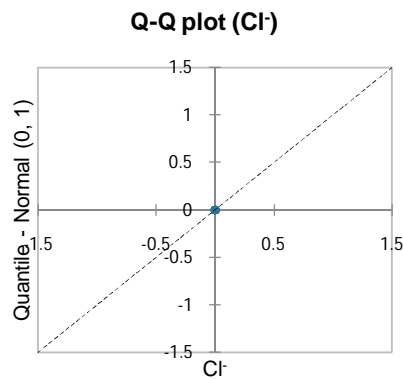


xxviii)

Figure 20: QQ-Plot for Sulphate in water samples collected near the dumpsites and control areas

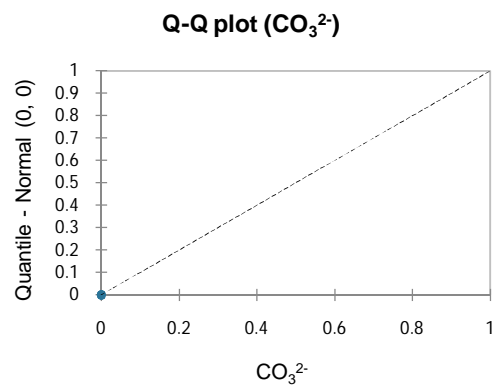
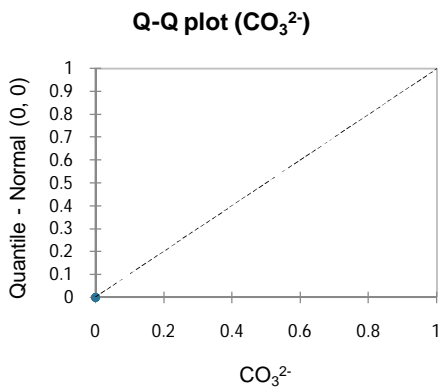


xxix)



xxx)

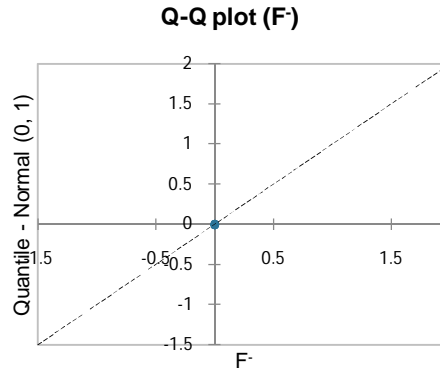
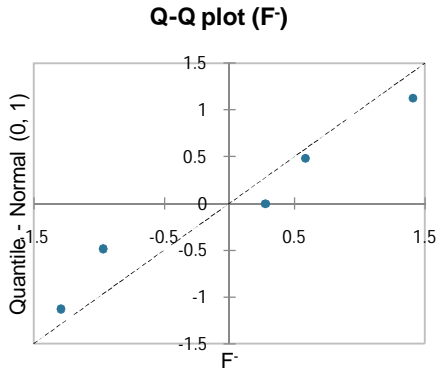
Figure 21: QQ-Plot for Chloride ions in water samples collected near the dumpsites and control areas



xxxii)

xxxii)

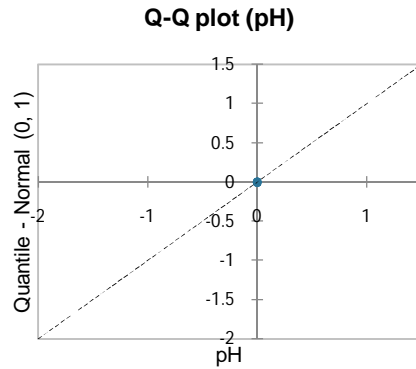
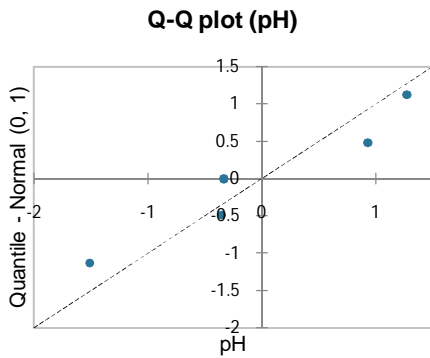
Figure 22: QQ-Plot for Carbonate in water samples collected near the dumpsites and control areas



xxxiii)

xxxiv)

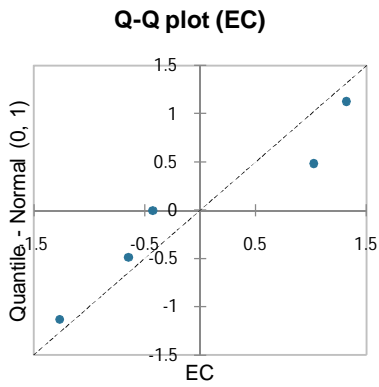
Figure 23: QQ-Plot for Fluoride in water samples collected near the dumpsites and control areas



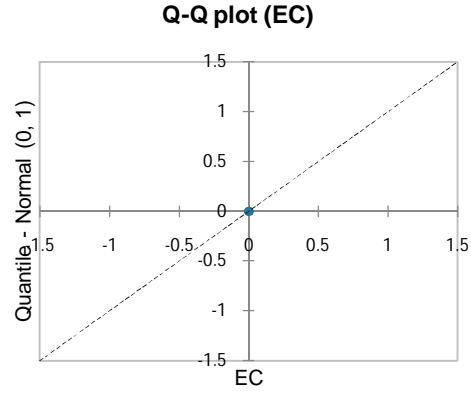
xxxv)

xxxvi)

Figure 24: QQ-Plot for pH in water samples collected near the dumpsites and control areas

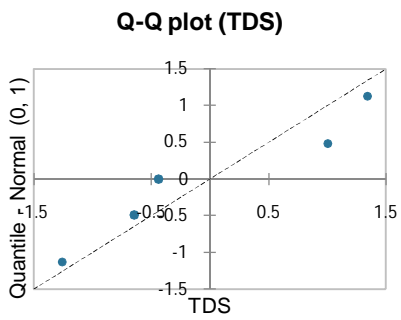


xxxvii)

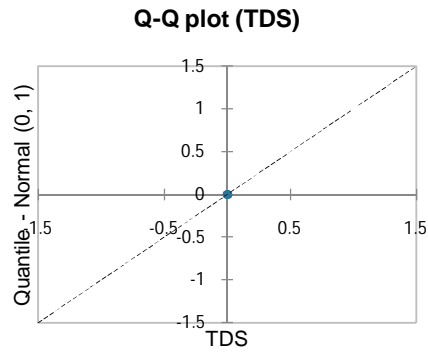


xxxviii)

Figure 25: QQ-Plot for EC in water samples collected near the dumpsites and control areas

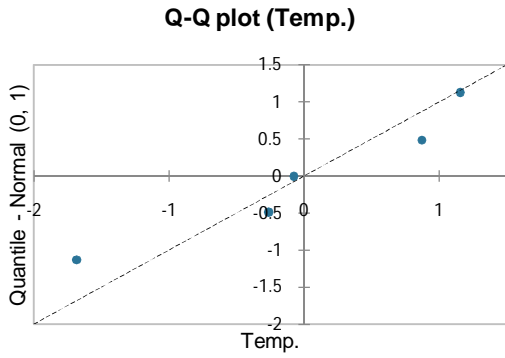


xxxix)

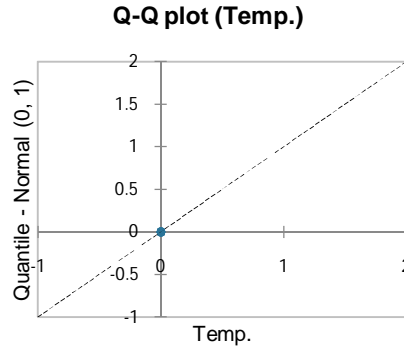


xxxx)

Figure 26: QQ-Plot for TDS in water samples collected near the dumpsites and control areas

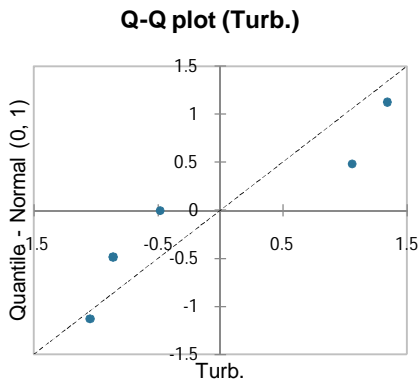


xxxxxi)

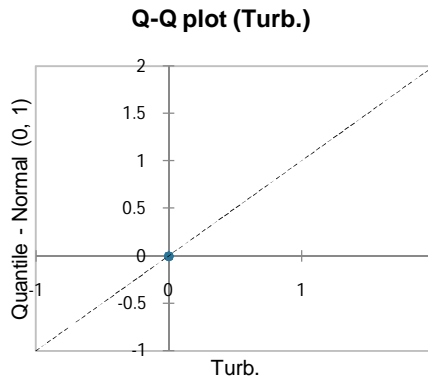


xxxix)

Figure 27: QQ-Plot for Temp. in water samples collected near the dumpsites and control areas

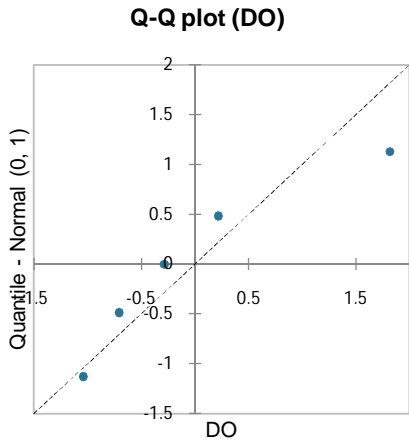


xxxix)

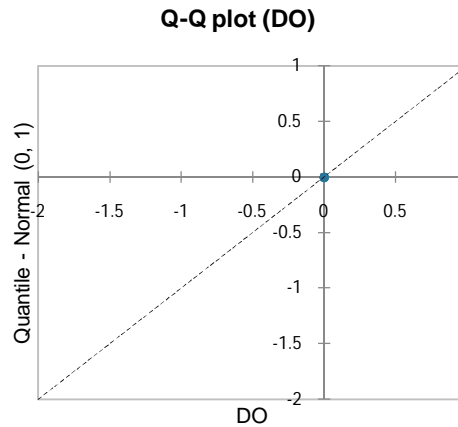


xxxix)

Figure 28: QQ- Plot for Turb. in water samples collected near the dumpsites and control areas

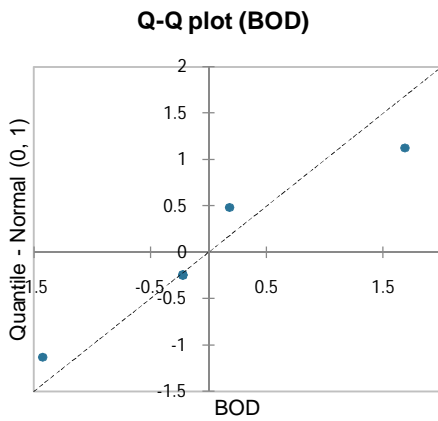


xxxxv)

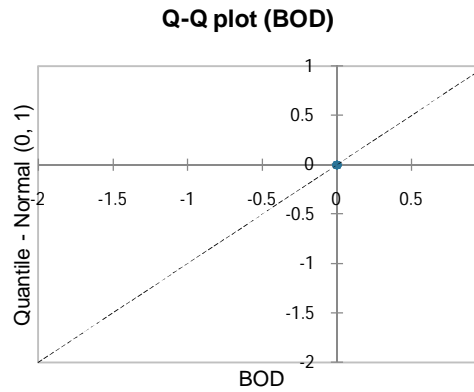


xxxxvi)

Figure 29: QQ-Plot for DO ions in water samples collected near the dumpsites and control areas



xxxxvi)



xxxxvii)

Figure 30: QQ-Plot for BOD in water samples collected near the dumpsites and control areas

4.1.1 Discussion

The discrimination analysis for water samples collected near the dumpsites and at the control areas presented in (Tables 3 and 4) revealed that the concentration of Ca^{2+} , K^+ , Mg^{2+} , Cu^{2+} , Na^+ , Fe^{2+} , Zn^{2+} , F^- , SO_4^{2-} , CO_3^{2-} , pH, EC, COD, DO and BOD are within permissible limits, while parameters such as Pb^{2+} which varies from (0.44 to 0.488 mg/l), Co^{2+} (0.226 to 0.44 mg/l), Mn^{2+} (20.73 to 27.144 mg/l), Cr^{2+} (1.28 to 1.68 mg/l) and Cd^{2+} (0.09 to 0.092 mg/l) exceeded this limits. The mean concentration of Ni^{2+} exceeded the standard permissible limits in water samples collected at the control areas while the mean concentration of Turbidity and Cl^- ion exceeded the

standard permissible limits for water samples collected near the dumpsites. The increased levels of toxic metals (Pb^{2+} , Co^{2+} , Mn^{2+} , Cr^{2+} , Cd^{2+} and Ni^{2+}) in both water sources could pose severe health hazards to the population.

a. Box plots

The box plots shown in (Figures 3 and 4) displayed side-by-side various water quality parameters for analysed water samples collected near dumpsite and the control areas, providing a quick visual comparison across several metrics. The size of the box (Interquartile range (IQR)) represents the spread of the middle 50 % of the data.

b. Scattergrams

The Scattergrams in (Figures 5 and 6) show how well the data points from one water source align with other parameters. The positive correlation (points aligning along a diagonal line) suggests similarity in the water quality parameters as correlated by the Principal Component Analysis (PCA).

c. Q-Q Plots

Q-Q plots shown in (Figure 7 - 30) help visualize how the distributions of the analysed parameters in water samples collected near the dumpsites differ with those collected near the control areas. As observed from the plots, the parameters of the Q-Q plots for both water sources follow a straight line, and therefore have identical distributions.

d. Ion dominance

The order of ion dominance for water samples collected near the dumpsites is:

$\text{K}^+ > \text{Ca}^{2+} > \text{Cu}^{2+} > \text{Ni}^{2+} > \text{Na}^+ > \text{Mn}^{2+} > \text{Mg}^{2+} > \text{Zn}^{2+} > \text{Co}^{2+} > \text{Cr}^{2+} > \text{Pb}^{2+} > \text{Cd}^{2+}$, while anions is in the order of $\text{F}^- > \text{SO}_4^{2-} > \text{Cl}^-$

This hierarchy suggests that K is the most dominant cation, followed by Ca^{2+} , Cu^{2+} and so on.

The order of ion dominance for water samples collected at the control sites is:

$\text{K}^+ > \text{Mn}^{2+} > \text{Ca}^{2+} > \text{Mg}^{2+} > \text{Cr}^{2+} > \text{Na}^+ > \text{Cu}^{2+} > \text{Co}^{2+} > \text{Zn}^{2+} > \text{Pb}^{2+} > \text{Cd}^{2+} > \text{Ni}^{2+}$ while Anions is in the order of $\text{Cl}^- > \text{SO}_4^{2-} > \text{F}^-$

This hierarchy suggests that K^{2+} is the most dominant cation, followed by Mn^{2+} , Ca^{2+} , Mg^{2+} and so on.

The ion dominance pattern in milli-equivalent indicates a natural water system with mineralogical influence, possibly with some anthropogenic input for metals and sulfate levels or geological materials such as feldspar or carbonate rocks as correlated by multivariate statistical analysis.

i. Bacteriological analysis

Table 3 presents bacteriological analysis results, showing Too Numerous To Count (TNTC) coliform counts in samples E, H, I. This were followed by samples D (79 cfu/ml), F (66 cfu/ml), B (39 cfu/ml), G (24 cfu/ml), and C (16 cfu/ml). All water samples tested negative for *E. coli*, *faecal strep*, and *Pseudomonas spp*, except for *Pseudomonas Spp* (02 cfu/ml) found in a hand-dug well at the Keffi control area. The bacteriological analysis revealed that all water sources had germ colonies above the WHO guideline, except a stream near the Karu dumpsite with Sample

ID A (9 cfu/ml) which fell within the WHO limit of 10 cfu/ml due to the dispersive continuous flow of the stream.

Table 3: Results of the Bacteriological analysis

S/N	SAMPLE ID	Coliforms (WHO, 2011) limit (10 cfu/ml)	<i>E. coli</i> (WHO, 2011) limit (0 cfu/ml)	<i>Faecal strep.</i> (WHO, 2011) limit (0 cfu/ml)	<i>Pseudomonas spp.</i> (WHO, 2011) limit (0 cfu/ml)
1	A	9	Nil	Nil	Nil
2	B	39	Nil	Nil	Nil
3	C	16	Nil	Nil	Nil
4	D	79	Nil	Nil	Nil
5	E	TNTC	Nil	Nil	2
6	F	66	Nil	Nil	Nil
7	G	24	Nil	Nil	Nil
8	H	TNTC	Nil	Nil	Nil
9	I	TNTC	Nil	Nil	Nil

Source: Laboratory analysis; TNTC = (Too Numerous To Count)

SAMPLE ID.

Stream under Karu-Abuja Bridge dumpsite (A); A borehole near Junior Sec. School (Karu-Abuja dumpsite control) (B); Stream adjacent Karu-Abuja dumpsite (C); a hand-dug well near Goshen control (D); Hand-Dug Well Keffi Control (E); a borehole Keffi control (F); a hand-dug well near Goshen dumpsite (G); a borehole near Tipper Garage dumpsite Karu-Abuja (H); and a borehole near Baptist Church dumpsite Panteka (I).

ii. WQI Analysis

The results of the computed Water Quality Index (WQI) and Heavy Metal Pollution Index (HPI) are shown in Table 4. The Water Quality Index (WQI) for water samples near dumpsites was 177.72, while samples from control areas were 62.25. This suggests that water samples collected near the dumpsites exhibited higher levels of contamination compared to those collected from the control areas. The overall Water Quality Index of water samples collected near the control sites suggests that are suitable for domestic uses. The WQI for F (42.92), B (47.17), D (54.2), I (69.3), H (74.77) were categorized as good and suitable for drinking, with F (42.92) and B (47.17), being the most suitable, while E (127.37), sample G (133.37), C (165.88), and Sample A (199.58) were classified as unsuitable for drinking.

iii. HPI Analysis

The computed HPI values are shown in Table 4. The water samples near dumpsites exhibited higher heavy metal pollution indices, with an overall HPI of 188.53, compared to 176.96 from control sites. The study indicates that both the water sources near dumpsites and control areas have a high heavy metal pollution index. The HPI for water sources near dumpsites shows higher levels of heavy metal contamination compared to control areas. The water samples collected from various locations were found to be highly impacted by leachate and intensive welding

activities. Sample H had the highest pollution index (HPI = 300.3), attributed to leachate infiltration and scavenger activities. Samples from C (220.98), A (181), E (165.14), B (162.5), I (104.74), F (102.8), and G (50.71) were classified as high heavy metal pollution indexes due to welding activities. The lowest pollution indices were found in samples from G (50.71) and D (25.14).

Table 4: Results of the Water Quality Index (WQI) and Heavy Metal Pollution Index (HPI)

S/N	SAMPLE ID.	WQI	Rating Class	HPI	Rating Class
1	A	199.58	Unsuitable for drinking	181	High heavy metal pollution
2	B	47.17	Good	162.5	High heavy metal pollution
3	C	165.88	Unsuitable for drinking	220.98	High heavy metal pollution
4	D	54.2	Poor	25.14	Low heavy metal Pollution
5	E	127.37	Unsuitable for drinking	165.14	High heavy metal pollution
6	F	42.92	Good	102.8	HM pollution on the threshold risk
7	G	133.37	Unsuitable for drinking	50.71	Low heavy metal Pollution
8	H	74.77	Very Poor	300.3	High heavy metal pollution
9	I	69.3	Poor	104.74	HM pollution on the threshold risk

Source: Laboratory analysis

e. Multivariate statistical analysis

i. Inter-elemental relationships between chemical parameters for water samples collected near dumpsites

The study reveals strong ($r > 0.8$) and moderate positive correlations ($r > 0.5-0.79$) between parameters in water samples near dumpsites, providing insights into water quality, pollution sources, and environmental interactions.

The strong correlation between EC-TDS (almost indistinguishable with $r = 1$) indicate the presence of dissolved salts or ions in water (Fu *et al.* 2024), while a strong correlation between Mn^{2+} and EC (0.985), suggests that Mn^{2+} contributes to the overall ionic content (Machado *et al.* 2024). The correlation between Mn^{2+} and Total Dissolved Solids (TDS) is strong ($r = 0.984$) indicating that Mn^{2+} is a significant component of the total dissolved solids in water. The correlation between DO and COD (0.983) indicates a strong connection between oxygen availability and organic/inorganic pollution levels (Meladet *et al.* 2024). The strong correlation between Mg^{2+} - Cl^- (0.969) indicates a common origin, possibly due to anthropogenic activities (Sghioueret *et al.* 2024). The strong correlation between BOD and COD (0.960) indicates a significant increase in oxygen consumption, potentially causing oxygen depletion and harming aquatic ecosystems (Melad et al. 2024). Pb^{2+} - Mg^{2+} (0.95) correlation is a common ion in water

due to their similarity in entering water through processes like mineral weathering or industrial discharge. A strong correlation between Pb^{2+} and Cl^- (0.92) suggests that Lead contamination may be linked to chloride, possibly from industrial processes, road salts, or saline intrusion. Pb^{2+} - Zn^{2+} (0.922) are common environmental metals, often found in areas impacted by mining, smelting, or industrial pollution, indicating a strong correlation between the two metals. The strong correlation between magnesium and BOD (0.915) suggests that magnesium may be linked to organic matter in water, possibly from agricultural runoff or wastewater. The strong correlation between magnesium and COD (0.913) indicates that magnesium may be linked to inorganic or organic pollutants that increase oxygen demand in water. The strong correlation between chloride and COD suggests that it may be linked to pollutants with high chemical oxygen demand, such as industrial waste or sewage. The strong correlation between Pb^{2+} - DO (0.892) suggests that lead's presence may impact water oxygen levels due to chemical reactions or pollution depleting oxygen. The correlation between potassium and BOD (0.883) indicates that potassium is strongly linked to organic matter in water (Sghioueret *al.* 2024). The correlation between BOD and chloride levels in water is strong BOD - Cl^- (0.87) indicating that organic pollution, as measured by BOD, is linked to chloride levels. Magnesium significantly influences water's ionic content, as indicated by a strong correlation between Mg and EC (0.857). which measures water's ability to conduct electricity based on dissolved ions. The correlation between Pb^{2+} -BOD (0.853) suggests that lead contamination may be linked to organic pollution. The correlation between Mg^{2+} and Total Dissolved Solids (TDS) is strong (0.85) indicating that magnesium significantly contributes to the total dissolved solids in water. The strong correlation between Zn^{2+} - Cl^- (0.844) suggests a shared source or similar behavior in the water system. The strong correlation between sodium levels and pH Na^+ - pH (0.836) indicates that the acidity or alkalinity of water may influence or affect sodium levels. The strong correlation between DO - Cl^- (0.831) suggests that chloride levels in water may be influencing dissolved oxygen levels, possibly due to pollution sources or chemical reactions. Parameters with moderate positive correlation ($r > 0.5$ – 0.79) were observed in Cr^{2+} - F^- (0.786), K^+ - DO (0.784), EC - Cl^- (0.778), SO_4^{2-} - Temp (0.775), K^+ - COD (0.776), Mn^{2+} - Cl^- (0.772), Ca^{2+} - TDS (0.771), TDS - Cl^- (0.77), Ca^{2+} - EC (0.762), Cd^{2+} - Cl^- (0.757), pH - F^- (0.754), Zn^{2+} - COD (0.748), Zn^{2+} - BOD (0.748), Mn^{2+} - BOD (0.74), K^+ - Temp. (0.733), Pb^{2+} - Mn^{2+} (0.730), Ca^{2+} - Mn^{2+} (0.728), Zn^{2+} - DO (0.678), Ca^{2+} - SO_4^{2-} (0.67), EC - BOD (0.662), TDS - BOD (0.652), Pb^{2+} - K^+ (0.604), Co^{2+} - Na^+ (0.631), K^+ - Mg^{2+} (0.657), pH - Temp. (0.653), Turb.- SO_4^{2-} (0.645), Na^+ - F^- (0.641), Mn^{2+} - COD (0.627), Mg^{2+} - Cd^{2+} (0.623), Cd^{2+} - EC (0.623), Cd^{2+} - TDS (0.622), Cu^{2+} - Fe^{2+} (0.6), Turb.- F^- (0.599), Na^+ - Turbidity (0.596), EC - COD (0.578), pH - SO_4^{2-} (0.57), TDS - COD (0.567), Co^{2+} - F^- (0.562), K^+ - Mn^{2+} (0.552), K^+ - Cl^- (0.539), Mn^{2+} - Cd^{2+} (0.535), Ca^{2+} - Zn^{2+} (0.526), Zn^{2+} - Cd^{2+} (0.522), Pb^{2+} - Cd^{2+} (0.519), Mn^{2+} - DO (0.502). This suggests that these chemical parameters originated from similar sources (geogenic or anthropogenic process) and can therefore have influence over one another (Meladet *al.* 2024).

Specifically, EC correlates with (TDS, DO, SO_4^{2-} , Temp, Cl^- and COD), while TDS correlates with (DO, SO_4^{2-} , Temp, Cl^- and COD). DO correlates with (BOD, SO_4^{2-} and COD). BOD correlates with (SO_4^{2-} and COD). Temp correlates with Cl^- . Cl^- correlates with COD. Ca^{2+} correlates with (Mn^{2+} , Zn, EC, TDS and SO_4^{2-}). Pb^{2+} correlates with (K^+ , Mg^{2+} , Mn^{2+} , Zn^{2+} ,

Cd²⁺, DO, BOD and Cl⁻). Co²⁺ correlates with Na⁺ and F⁻. K⁺ correlates with (Mg²⁺, Mn²⁺, DO, BOD, Temp. Cl⁻, and COD).

Mg²⁺ correlates with Mn²⁺, Zn²⁺, Cd²⁺, EC, TDS, BOD, Temp. Cl⁻ and COD. Cu²⁺ correlates with Fe. Mn²⁺ correlates with Zn²⁺, Cd, EC, TDS DO, BOD, Cl⁻ and COD; Na⁺ correlates with pH, Turbidity and F⁻. Cr²⁺ correlates with F⁻. Zn²⁺ correlates with Cd²⁺, EC, TDS, DO, BOD, Cl⁻ and COD. Cd²⁺ correlates with EC, TDS and Cl⁻. pH correlates with Turbidity, F⁻, SO₄²⁻ and Temp. EC correlates with TDS, F⁻, SO₄²⁻ and COD. TDS correlates with BOD, Cl⁻ and COD. Turbidity correlates with F⁻, SO₄²⁻ and Temp. DO correlates with Cl⁻ and COD. BOD correlates with Cl⁻ and COD. SO₄²⁻ correlates with Temp. Cl⁻ correlates with COD. The correlation between chemical parameters around the control sites suggests that these parameters share common origin and similar sources attributed to mineral deposits, percolation of organic and inorganic pollutants into the subsurface, agricultural activities and discharges from poorly treated sewage which often contain high levels of dissolved solids (TDS), organics (increasing COD), and salts like Mg and Cl (Gyabaahet *al.* 2024).

ii. Inter-elemental relationships between chemical parameters for water samples collected from control sites

The water samples collected at control areas show a strong positive correlation between EC-TDS, almost indistinguishable with a $r = 1$ value. Other parameters with strong positive correlation with ($r > 0.8$) include: The strong positive correlation between Ni²⁺ -Temp. (0.999). This suggests that higher temperatures may facilitate the dissolution or mobility of Ni in water or from industrial or natural sources. The correlation between Ca²⁺ - EC (0.999) indicates that an increase in Ca²⁺ concentration also enhances the water's ability to conduct electricity. A strong correlation between Ca²⁺ -TDS (0.999) indicates that Ca is a major component of dissolved solids in the water in areas with hard water or limestone geology. DO - COD (0.997), Na⁺ - Temp. (0.985). A strong correlation between Na and temperature could indicate that higher temperatures increase solubility or mobility of Na in water, either from natural weathering processes or anthropogenic sources such as industrial effluents or road salt runoff. Others include: Mn²⁺- Cl⁻ (0.989), Pb²⁺ - Temp. (0.983), Ni²⁺ - Na⁺ (0.982). A strong correlation between Na and Ni could indicate that both Ni and Na share a common source, such as industrial pollution or groundwater contamination. Pb²⁺ - Ni²⁺ (0.976), DO-BOD (0.974), Ca²⁺ - Mn²⁺ (0.971), Mn²⁺- EC (0.965), Mn²⁺—TDS (0.965), Ca²⁺ - Cl⁻ (0.96), BOD-COD (0.954), TDS - Cl⁻ (0.951), EC - Cl⁻ (0.951), Pb²⁺ - Cl⁻ (0.947), K⁺ - F⁻ (0.94), Pb²⁺ - Mn²⁺ (0.922), Mg²⁺ - EC (0.922), Mg²⁺ - TDS (0.923), Mg²⁺ - SO₄²⁻ (0.953), Na⁺ - Cl⁻ (0.928). Mn²⁺ - Na⁺ (0.919), Cd²⁺ - F⁻ (0.917), Ca²⁺ - Mg²⁺ (0.916), pH - COD (0.9), pH - BOD (0.893), Cr²⁺ - Zn²⁺ (0.888), Ca²⁺ - Pb²⁺ (0.821), Ca²⁺- Na⁺ (0.802), Pb²⁺ - EC (0.804), Pb²⁺- TDS (0.804), Co²⁺ - Cu²⁺ (0.818), Ni²⁺ - Mn²⁺ (0.831), Ni²⁺ - Cl⁻ (0.856), K⁺ - Cd (0.898), Temp - Cl⁻ (0.871), Mn²⁺ - Temp. (0.845). Parameters with moderate positive correlation ($r > 0.5-0.79$) were observed in Co- F⁻ (0.799), Mg²⁺ - Cl⁻ (0.796), Mg²⁺ - Mn²⁺ (0.795), SO₄²⁻ - COD (0.79), Na⁺ - EC (0.786), Na⁺ - TDS (0.785), TDS - SO₄²⁻ (0.768), EC - SO₄²⁻ (0.767), Ca²⁺ - SO₄²⁻ (0.761) (suggests that the calcium in groundwater is not only from calcium sulfate minerals but also from other sources such as weathering of carbonate rocks). DO - SO₄²⁻ (0.747), Cu²⁺ - F⁻ (0.732), Mg²⁺ - COD (0.715), Ca²⁺ - Temp. (0.706), Ca²⁺ - Ni (0.685), TDS-Temp. (0.685), EC - Temp. (0.685), Pb²⁺ - pH (0.677), Cr²⁺ - SO₄²⁻ (0.662), Ni²⁺ - EC (0.665), pH -Temp. (0.65), Ni²⁺ - TDS (0.664), BOD - SO₄²⁻ (0.636), Cl⁻ - COD (0.628), K⁺ - Cu²⁺ (0.623), SO₄²⁻ - Cl⁻ (0.617), pH - Cl⁻ (0.624), Ni - pH (0.637), Ni²⁺ - Cu²⁺ (0.609), Ca²⁺ - COD (0.608), Co²⁺ - Cd²⁺ (0.599), TDS - COD (0.595), Cu²⁺

- Temp (0.593), EC - COD (0.593), Mn^{2+} - SO_4^{2-} (0.591), Mg^{2+} - Cr^{2+} (0.588), Na^+ - pH (0.58), DO - Cl^- (0.578), Pb^{2+} - Mg^{2+} (0.565), Co^{2+} - K (0.557), Ca^{2+} - DO (0.546), Pb^{2+} - COD (0.538), TDS - DO (0.531), EC - DO (0.529), Mn^{2+} - COD (0.525), Pb^{2+} - Cu^{2+} (0.52), Mg^{2+} - Na^+ (0.514), Pb^{2+} - DO (0.503). The correlation between chemical parameters around the control sites suggests that these parameters share common origin and similar sources attributed to geogenic or anthropogenic process. This can provide valuable insights into water treatment needs, potential impacts on human and environmental health (Nayaket *al.* 2024).

Generally, Ca^{2+} correlates with (Pb^{2+} , Ni^{2+} , Mg^{2+} , Mn^{2+} , Na^+ , EC, TDS, DO, SO_4^{2-} , Temp, Cl^- and COD). This suggests that Ca^{2+} originated from the dissolution of salts in groundwater. Pb^{2+} correlates with (Ni , Mg^{2+} , Cu^{2+} , Mn^{2+} , Na^+ , pH, EC, TDS, DO, Temp, Cl^- , COD). Co^{2+} correlates with (K^+ , Cu^{2+} , Cd^{2+} , and F^-). Ni^{2+} correlates with Cu^{2+} , Mn^{2+} , Na^+ , pH, EC, TDS Temp. and Cl^-). K^+ correlates with Cu^{2+} , Cd^{2+} and F^- . Mg^{2+} correlates with (Mn^{2+} , Na^+ , Cr^{2+} , EC, TDS, DO, SO_4^{2-} , Cl^- and COD), these values suggest the participation of both carbonate and silicate minerals during the weathering process. Cu^{2+} correlates with Na, F, and Temp. Mn^{2+} correlates with Na^+ , pH, EC, TDS, SO_4^{2-} , Temp, Cl^- and COD. Na^+ correlates with pH, EC, TDS, Temp. and Cl^- . Cr^{2+} correlates with Zn and SO_4^{2-} . Cd correlates with F^- . pH correlates with DO, BOD, SO_4^{2-} , Temp. and COD. EC correlates with TDS, DO, SO_4^{2-} , Temp., Cl^- and COD. TDS correlates with DO, SO_4^{2-} , Temp, Cl^- and COD. DO correlates with BOD, SO_4^{2-} , and COD. SO_4^{2-} correlates with Cl^- and COD. Temp. correlates with Cl^- . Cl^- correlates with COD as shown Tables 5 and 6:

Table 5: Matrix of correlation for water variables collected near dumpsites

Parameters	Ca	Pb	Co	K	Mg	Cu	Mn	Na	Cr	Fe	Zn	Cd	pH	EC	TDS	Turb	DO	BOD	F	SO4	Temp	Cl	COD	
Ca	1																							
Pb	0.162	1																						
Co	-0.015	-0.186	1																					
K	-0.002	0.604	-0.387	1																				
Mg	0.324	0.950	-0.426	0.657	1																			
Cu	0.140	-0.474	-0.670	-0.356	-0.227	1																		
Mn	0.728	0.730	-0.380	0.552	0.871	-0.058	1																	
Na	0.011	-0.835	0.631	-0.490	-0.883	-0.025	-0.612	1																
Cr	-0.884	-0.012	0.160	0.339	-0.195	-0.472	-0.550	0.054	1															
Fe	-0.621	-0.183	-0.571	-0.244	-0.140	0.600	-0.414	-0.336	0.230	1														
Zn	0.526	0.922	-0.105	0.511	0.927	-0.405	0.894	-0.681	-0.337	-0.441	1													
Cd	0.291	0.519	-0.551	-0.085	0.623	0.405	0.535	-0.779	-0.558	0.397	0.522	1												
pH	-0.147	-0.594	0.503	0.049	-0.650	-0.288	-0.473	0.836	0.410	-0.443	-0.535	-0.982	1											
EC	0.762	0.730	-0.323	0.417	0.857	-0.040	0.985	-0.614	-0.636	-0.393	0.910	0.623	-0.562	1										
TDS	0.771	0.723	-0.315	0.405	0.850	-0.038	0.984	-0.605	-0.646	-0.399	0.907	0.622	-0.560	1.000	1									
Turb	-0.119	-0.398	0.218	0.392	-0.391	-0.260	-0.238	0.596	0.452	-0.426	-0.368	-0.906	0.927	-0.374	-0.376	1								
DO	-0.210	0.892	-0.336	0.784	0.837	-0.449	0.502	-0.829	0.371	0.046	0.678	0.315	-0.426	0.446	0.434	-0.162	1							
BOD	0.089	0.853	-0.541	0.883	0.915	-0.236	0.740	-0.831	0.108	-0.059	0.748	0.378	-0.421	0.662	0.651	-0.084	0.919	1						
F	-0.706	-0.516	0.562	-0.147	-0.711	-0.383	-0.848	0.641	0.786	0.023	-0.683	-0.844	0.754	-0.892	-0.893	0.599	-0.245	-0.488	1					
SO4	0.670	-0.078	0.223	0.336	0.020	-0.213	0.413	0.417	-0.299	-0.860	0.213	-0.461	0.570	0.341	0.345	0.645	-0.201	0.057	-0.080	1				
Temp.	0.145	0.149	0.168	0.733	0.148	-0.539	0.265	0.202	0.319	-0.691	0.207	-0.648	0.653	0.130	0.126	0.832	0.266	0.374	0.247	0.775	1			
Cl	0.196	0.921	-0.519	0.539	0.969	-0.097	0.772	-0.967	-0.178	0.092	0.844	0.757	-0.798	0.778	0.770	-0.559	0.831	0.870	-0.725	-0.215	-0.073	1		
COD	-0.072	0.920	-0.447	0.776	0.913	-0.328	0.627	-0.899	0.207	0.054	0.748	0.448	-0.533	0.578	0.567	-0.248	0.983	0.960	-0.416	-0.171	0.211	0.911	1	

Significance bold values are $p < 0.5$

Table 6: Matrix of correlation for water variables collected around the control sites

Parameters	Ca	Pb	Co	Ni	K	Mg	Cu	Mn	Na	Cr	Zn	Cd	pH	EC	TDS	Turb	DO	BOD	F	SO4	Temp	Cl	COD	
Ca	1																							
Pb	0.821	1																						
Co	-0.262	0.154	1																					
Ni	0.685	0.976	0.339	1																				
K	-0.148	-0.269	0.557	-0.222	1																			
Mg	0.916	0.565	-0.615	0.373	-0.268	1																		
Cu	0.305	0.520	0.818	0.609	0.623	-0.063	1																	
Mn	0.971	0.922	-0.041	0.831	-0.105	0.795	0.483	1																
Na	0.802	0.992	0.258	0.982	-0.149	0.514	0.625	0.919	1															
Cr	0.308	-0.289	-0.672	-0.476	0.230	0.588	-0.328	0.094	-0.304	1														
Zn	-0.116	-0.653	-0.726	-0.801	0.103	0.255	-0.641	-0.344	-0.686	0.888	1													
Cd	-0.567	-0.575	0.599	-0.471	0.898	-0.639	0.399	-0.512	-0.465	0.033	0.113	1												
pH	0.483	0.677	-0.328	0.637	-0.890	0.445	-0.219	0.504	0.583	-0.342	-0.411	-0.948	1											
EC	0.999	0.804	-0.269	0.665	-0.126	0.922	0.304	0.965	0.786	0.336	-0.090	-0.549	0.457	1										
TDS	0.999	0.804	-0.271	0.664	-0.127	0.923	0.302	0.965	0.785	0.337	-0.089	-0.550	0.458	1.000	1									
Turb	-0.931	-0.611	0.240	-0.459	-0.167	-0.886	-0.361	-0.869	-0.620	-0.551	-0.113	0.278	-0.138	-0.942	-0.942	1								
DO	0.546	0.503	-0.677	0.386	-0.901	0.657	-0.476	0.467	0.389	0.049	-0.013	-0.995	0.914	0.529	0.531	-0.276	1							
BOD	0.343	0.340	-0.693	0.244	-0.969	0.493	-0.619	0.262	0.217	-0.022	0.022	-0.962	0.893	0.325	0.327	-0.061	0.974	1						
F	-0.286	-0.201	0.799	-0.086	0.940	-0.499	0.732	-0.169	-0.074	-0.115	-0.192	0.917	-0.802	-0.273	-0.275	0.046	-0.946	-0.985	1					
SO4	0.761	0.360	-0.824	0.153	-0.425	0.953	-0.362	0.591	0.281	0.662	0.445	-0.705	0.467	0.767	0.768	-0.722	0.747	0.636	-0.679	1				
Temp.	0.706	0.983	0.310	0.999	-0.236	0.402	0.593	0.845	0.985	-0.453	-0.782	-0.492	0.650	0.685	0.685	-0.479	0.409	0.265	-0.109	0.184	1			
Cl	0.960	0.947	-0.096	0.856	-0.245	0.796	0.397	0.989	0.928	0.031	-0.377	-0.624	0.624	0.951	0.951	-0.811	0.578	0.389	-0.290	0.617	0.871	1		
COD	0.608	0.538	-0.683	0.410	-0.863	0.715	-0.437	0.525	0.427	0.098	0.002	-0.991	0.900	0.593	0.595	-0.352	0.997	0.954	-0.927	0.790	0.434	0.628	1	

Significance bold values are $p < 0$.

f. Groundwater types and evaluation

The hydrochemicalfacies of groundwater explains the relation between major anions and cations and their behaviour. Hydrochemicalfacies help in establishing the classification of different water types (Piper, 1994) and in understanding the origin and geochemical evolution of groundwater.

i. Piper Trilinear plot

ii. Facie for water samples collected near the dumpsites

The piper diagram (Figure 31A) shows Ca-Mg-HCO₃ (20%) and Ca-Mg- SO₄ (60%) mixed water type for samples near the dumpsites, which is mainly influenced by the recharged water from the streams or perhaps caused by rock-water interaction associated with intermediate EC values. Also, the dissolution of dolomite and calcite may cause this water type. The plotted cations indicate the dominance of Ca²⁺ and Mg²⁺, and in anions, CO₃⁻ and SO₄²⁻ dominance indicating temporary hardness.

iii. Facie for water samples collected around the control sites

Piper diagrams (Figure 31B) shows Ca-Mg-HCO₃ (40%) and Ca-Mg- SO₄ (90%) mixed water type for samples near the control areas. The plotted cations indicate the dominance of Ca²⁺ and Mg²⁺ and in the anion plot, CO₃⁻ and SO₄²⁻ indicating temporary hardness.

iv. Durov plot

The Durov plot of the water samples indicates that there are mainly two geochemical processes that could affect the genesis of water in the study area (Figures 32A and 32 B) Samples from dumpsites show HCO_3^- and Ca^{2+} dominance (60 %) and control sites (86 %), suggesting mixing, uncommon dissolution influences, and reverse ion exchange processes.

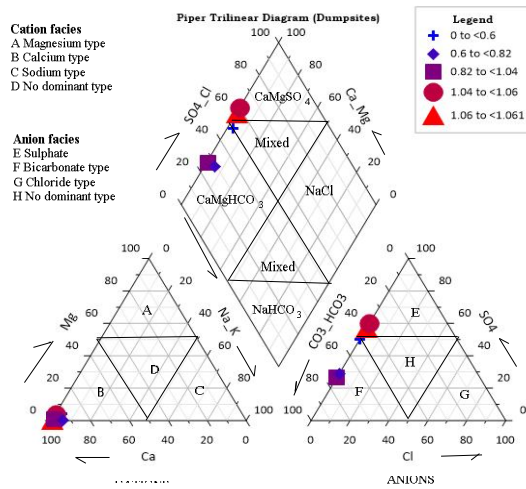


Figure 31(A):

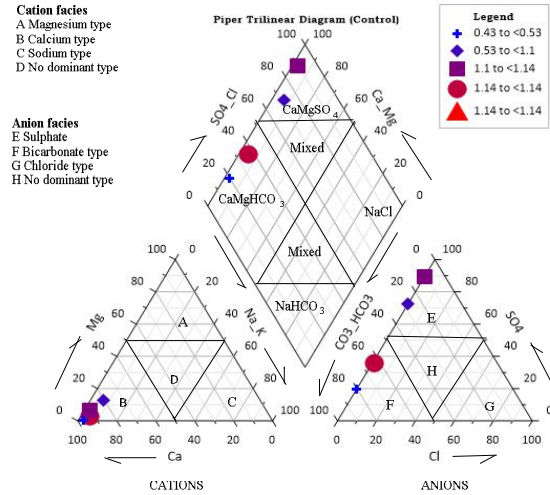


Figure 31(B):

Figures 31(A-B): Piper trilinear diagram showing the hydrochemical characteristics and hydrochemicalfacies of water samples collected near the dumpsites and control sites

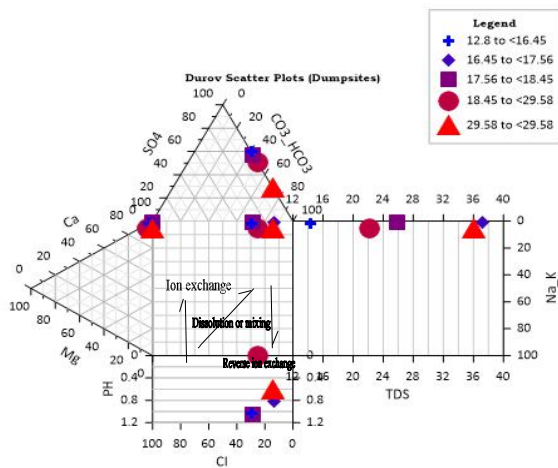


Figure 32(A):

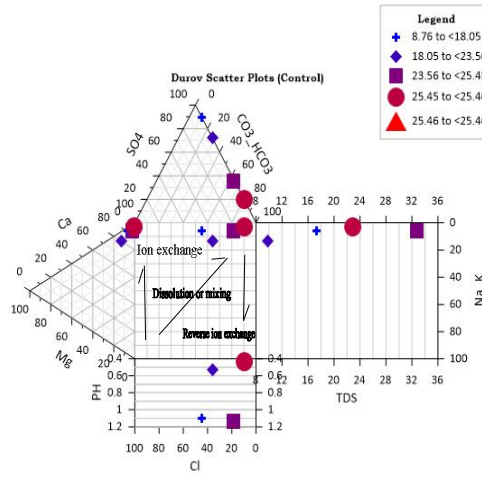


Figure 32(B):

Figures 32(A-B): Durov diagram showing the dominant chemical processes affecting groundwater chemistry near dumpsites and control sites

g. Comparative Analysis of Principal Components Analysis (PCA)

The Principal component analysis (PCA) results comparing the 3-D tri-plots and scree plots for the analysed water samples collected near the Dumpsites and samples collected around the control sites are shown in figures 33 to 34:

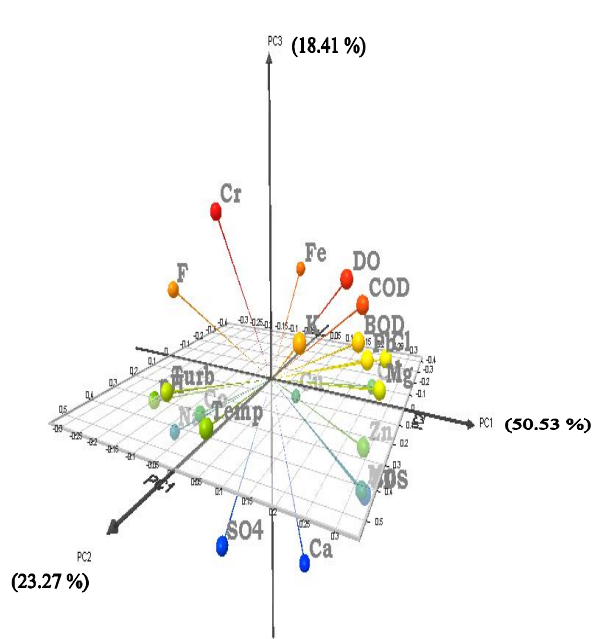


Figure 33(A):

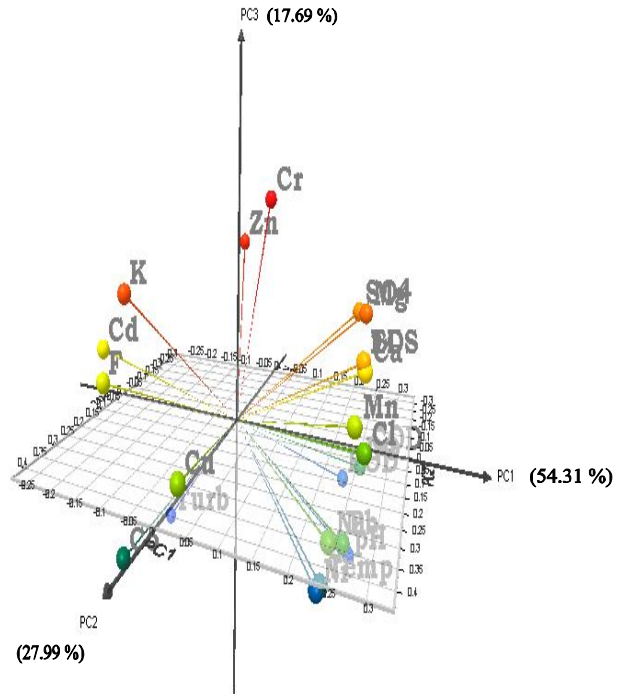


Figure 33(B):

Figures 33(A-B): 3-D tri-plots score showing PC1, PC2 and PC3 for: water samples collected near dumpsites and analysed water samples collected near control sites.

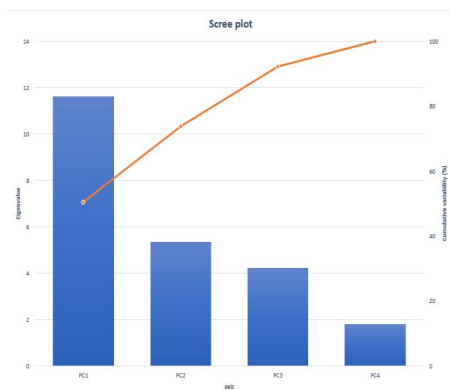


Figure 34(A):

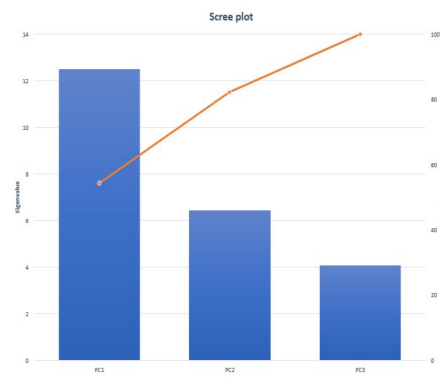


Figure 34(B):

Figures 34(A-B): 3-D bar-plots score showing PC1, PC2 and PC3 for: water samples collected near dumpsites and analysed water samples collected near control sites.

Table 7: Extracted Principal Components and their total variance for water samples collected within dumpsites

Loadings	PC1 (50.527%)	PC2 (23.269%)	PC3 (18.407%)	PC4 (7.797%)
Ca ²⁺	0.119	0.082	-0.434	-0.021
Pb ²⁺	0.263	0.086	0.126	0.221
Co ²⁺	-0.146	0.162	-0.075	0.572
K ⁺	0.160	0.274	0.192	-0.285
Mg ²⁺	0.288	0.062	0.055	0.026
Cu ²⁺	-0.021	-0.300	-0.154	-0.481
Mn ²⁺	0.262	0.111	-0.171	-0.083
Na ⁺	-0.263	0.109	-0.178	0.033
Cr ²⁺	-0.101	0.124	0.435	0.018
Fe ²⁺	-0.021	-0.351	0.242	-0.219
Zn ²⁺	0.266	0.122	-0.062	0.216
Cd ²⁺	0.218	-0.283	-0.064	0.044
pH	-0.219	0.279	-0.015	-0.114
EC	0.263	0.065	-0.201	0.005
TDS	0.262	0.064	-0.207	0.009
Turb.	-0.148	0.329	0.039	-0.299
DO	0.218	0.104	0.302	0.039
BOD	0.251	0.129	0.175	-0.168

F ⁻	-0.242	0.119	0.229	0.117
SO ₄ ²⁻	-0.005	0.337	-0.284	-0.165
Temp	0.003	0.419	0.028	-0.177
Cl ⁻	0.286	-0.038	0.098	0.031
COD	0.248	0.075	0.244	-0.012
Eigen values	11.621	5.352	4.234	1.793
Variability (%)	50.527	23.269	18.407	7.797
Cumulative (%)	50.527	73.796	92.203	100.000

Table 8: Extracted Principal Components and their total variance for water samples collected within control sites

Loadings	PC1 (54.313%)	PC2 (27.993%)	PC3 (17.693%)
Ca ²⁺	0.257	0.084	0.177
Pb ²⁺	0.24	0.19	-0.09
Co ²⁺	-0.107	0.346	-0.144
Ni ²⁺	0.208	0.237	-0.156
K ⁺	-0.152	0.236	0.295
Mg ²⁺	0.242	-0.067	0.243
Cu ²⁺	0.018	0.391	0.051
Mn ²⁺	0.251	0.161	0.106
Na ⁺	0.225	0.234	-0.065
Cr ²⁺	0.025	-0.170	0.445
Zn ²⁺	-0.064	-0.277	0.334
Cd ²⁺	-0.240	0.166	0.159
pH	0.227	-0.084	-0.278
EC	0.254	0.083	0.192
TDS	0.254	0.082	0.192
Turb	-0.199	-0.099	-0.330
DO	0.233	-0.198	-0.132
BOD	0.191	-0.246	-0.193
F ⁻	-0.170	0.293	0.143
SO ₄ ²⁻	0.218	-0.181	0.219
Temp	0.214	0.229	-0.148
Cl ⁻	0.266	0.130	0.051
COD	0.243	-0.186	-0.099
Eigen values	12.492	6.438	4.069
Variability (%)	54.313	27.993	17.693
Cumulative(%)	54.313	82.307	100.000

Table 9: The Kaiser-Meyer-Olkin measure of sampling the adequacy for water samples collected near the dumpsites

Variable	KMO sampling adequacy
Ca ²⁺	0.424
Pb ²⁺	0.609
Co ²⁺	0.406
Ni ²⁺	0.000
K ⁺	0.484
Mg ²⁺	0.724
Cu ²⁺	0.346
Mn ²⁺	0.641
Na ⁺	0.664
Cr ²⁺	0.417
Zn ²⁺	0.638
Cd ²⁺	0.667
pH	0.605
EC	0.653
TDS	0.649
Turb.	0.465
DO	0.562
BOD	0.614
F ⁻	0.629
SO ₄ ²⁻	0.388
Temp.	0.445
Cl ⁻	0.686
COD	0.611
KMO	0.574
Cronbach's alpha	0.693

Table 10: The Kaiser-Meyer-Olkin measure of sampling the adequacy for water samples collected near the control centres

Variable	KMO sampling adequacy
Ca ²⁺	0.567
Pb ²⁺	0.614
Co ²⁺	0.493
Ni ²⁺	0.561
K ⁺	0.424
Mg ²⁺	0.554
Cu ²⁺	0.428
Mn ²⁺	0.579

Na ⁺	0.591
Cr ²⁺	0.303
Zn ²⁺	0.384
Cd ²⁺	0.577
pH	0.514
EC	0.557
TDS	0.558
Turb.	0.454
DO	0.581
BOD	0.503
F ⁻	0.503
SO ₄ ²⁻	0.561
Temp.	0.569
Cl ⁻	0.633
COD	0.614
KMO	0.534
Cronbach's alpha	0.811

i. PCA for water samples collected near dumpsites

PC1 for water samples collected around the dumpsites explains approximately (50.527% of the total variance, eigenvalue of 11.62) and has strong positive correlation value with Mg²⁺ and Cl⁻ and a moderately positive correlation with Pb²⁺, Mn²⁺, Zn²⁺, Cd²⁺, DO, BOD and COD which reflects the role of lithogenic and anthropogenic factors in influencing the water chemistry. Strong correlation of Cl⁻ ions with alkali and alkaline earth metals Mg, indicated the natural weathering sources.

PC2 (23.269% of total variance, eigenvalue of 5.35) has strong positive correlation with Temperature, SO₄²⁻, and Turb. Has moderate positive correlation with pH and K⁺ and strong negative correlation with Cu²⁺ and Fe²⁺. The significant inverse relationship between Cu²⁺ and Fe²⁺ indicates the diverse source of chemical origin.

PC3 (18.407% of total variance, eigenvalue of 4.23) was strongly positive weighted on Cr²⁺ and DO, and moderate positive score on COD and F⁻.

PC4 explains (7.797% of the total variance, eigenvalue of 1.79) observed and has strong positive correlation with Co²⁺ and a moderately strong positive correlation with Zn²⁺. It has strong negative correlation with Cu²⁺, Turbidity and K⁺.

ii. PCA for water samples collected near the control sites

PC1 for water samples collected around the control sites explains approximately (54.3 % of the total variance, eigenvalue of 12.49), and has strong positive correlation value with Ca²⁺, Cl⁻ and EC, Mn²⁺, COD, Pb²⁺ Mg²⁺, Na⁺, DO, SO₄²⁻, pH and TDS which reflects the role of lithogenic factors in influencing the water chemistry, and a moderately strong positive correlation with Temp. and Ni²⁺. Strong correlation of Cl⁻ ions with alkali and alkaline earth metals Mg²⁺,

indicated the natural weathering sources. A high positive loading of Ca^{2+} , Na^+ and Cl^- and SO_4^{2-} , is attributed to various natural processes such as - weathering of rock minerals (limestone and calcium carbonate bearing rocks) and to various ion-exchange processes taking place in the groundwater system.

PC2 (23.269% of total variance, eigenvalue of 6.44) has strong positive correlation with Cu^{2+} and Co^{2+} , has moderate positive correlation with Ni^{2+} , K^+ , F^- and Temperature and strong negative correlation with Zn^{2+} and BOD.

PC3 (17.693% of total variance, eigenvalue of 4.07) was strongly positive weighted on Cr^{2+} and Zn^{2+} and moderate positive score on K^+ , Mg^{2+} and SO_4^{2-} and strong negative correlation with Turbidity and pH, hence, diverse origin.

h. Limitations/Recommendations

The study suggests that despite not conclusively proving *faecal strep. and E. coli* contamination in samples, it suggests the need for continuous monitoring of water sources in these areas.

5. CONCLUSION

This study evaluated and compared the physicochemical and bacteriological parameters in water sources located near major dumpsites and control areas in Karu-Abuja and parts of Nasarawa State, using multivariate statistical analysis, indexing approach, Principal Component Analysis and hydrochemical facie analysis. Twenty-five physico-chemical and four bacteriological parameters from nine water samples collected from boreholes, hand-dug wells and streams were analysed to determine the extent of environmental pollution and potential health risks using the Atomic Absorption Spectrophotometry (AAS), colorimetric and standard techniques alluded by APHA. The data were analysed with the aid of Grapher, Surfer and XLSTAT statistical tools. Discrimination analysis revealed that the concentration of Ca^{2+} , K^+ , Mg^{2+} , Cu^{2+} , Na^+ , Fe^{2+} , Zn^{2+} , F^- , SO_4^{2-} , CO_3^{2-} , pH, EC, COD, DO and BOD are within permissible limits, while parameters such as Pb^{2+} which varies from (0.44 to 0.488 mg/l), Co^{2+} (0.226 to 0.44 mg/l), Mn^{2+} (20.73 to 27.144 mg/l), Cr^{2+} (1.28 to 1.68 mg/l) and Cd^{2+} (0.09 to 0.092 mg/l) exceeded this limits. The mean concentration of Ni^{2+} exceeded the standard permissible limits in water samples collected at the control areas while the mean concentration of Turbidity and Cl^- ion exceeded the standard permissible limits for water samples collected near the dumpsites. The increased levels of toxic metals (Pb^{2+} , Co^{2+} , Mn^{2+} , Cr^{2+} , Cd^{2+} and Ni^{2+}) in both water sources could pose severe health hazards to the population. The overall WQI evaluation for water samples collected near the dumpsites was 177.72, while samples collected at the control sites was 62.25. This suggests that water samples collected near the dumpsites exhibited higher levels of contamination compared to samples collected from the control areas. Results also revealed that only the water samples collected from boreholes located at the control areas were suitable for domestic purposes with (WQI < 48), in contrast to water samples from streams and hand-dug wells situated near the dumpsites with (WQI > 100). The overall HPI for water samples collected near the dumpsites was 188.53, while samples collected from the control sites was 176.96, indicating higher heavy

metal pollution indices for water sources near the dumpsites. Bacteriological analysis showed that the coliform count for water samples collected from boreholes situated near the dumpsites were Too Numerous To Count (TNTC), while samples from the streams revealed the lowest coliform counts of (9 to 16 cfu/ml), attributed to continuous flow which disperses bacteria. There was no detection of *E. coli*, faecal strep and *Pseudomonas* spp in all the water samples, except (02 cfu/ml) *Pseudomonas* Spp detected in a hand-dug well at the Keffi control area. The decreasing order of dominance for major cations and anions near dumpsites include: $K^+ > Ca^{2+} > Cu^{2+} > Ni^{2+} > Na^+ > Mn^{2+} > Mg^{2+} > Zn^{2+} > Co^{2+} > Cr^{2+} > Pb^{2+} > Cd^{2+}$, and in anions: $F^- > SO_4^{2-} > Cl^-$, while control sites showed: $K^+ > Mn^{2+} > Ca^{2+} > Mg^{2+} > Cr^{2+} > Na^+ > Cu^{2+} > Co^{2+} > Zn^{2+} > Pb^{2+} > Cd^{2+} > Ni^{2+}$ and in anions: $Cl^- > SO_4^{2-} > F^-$, attributed to agricultural practices, smelting, septic tanks, leaching and weathering. Three Principal components (PCs) explained 92.2 % and 95.3 % of the total variance of water samples near the dumpsites and control sites respectively. Piper trilinear and Durov diagram reflects mixed water types Ca-Mg-HCO₃ and Ca-Mg-SO₄ for both water samples, indicating temporary hardness. The findings emphasised the importance of regular water testing and the siting of boreholes and hand-dug wells at safe distances from potential contamination sources to safeguard public health.

Authors' contributions

This work was carried out in collaboration among all authors. All authors read and approved the final manuscript.

Disclaimer (Artificial intelligence)

Author(s) hereby declare that NO generative AI technologies such as Large Language Models (ChatGPT, COPILOT, etc.) and text-to-image generators have been used during the writing or editing of this manuscript.

REFERENCES

- Abdu-Raheem, Y. A., Oyebamiji, A. O., Afolagboye, L. O., & Talabi, A. O. (2024). Assessment of ecological and health risk impact of heavy metals contamination in stream sediments in Itapaji-Ekiti, SW Nigeria. *Journal of Trace Elements and Minerals*, 8, 100121.
- Adeleke, I. F., & Faraday, E. T. (2024). Assessment of the Microbial and Physicochemical Quality of Water: Evidence from Selected Groundwater Sources from The Coastal Region of Ondo State, Nigeria. DOI: <https://dx.doi.org/10.4314/dujopas.v10i1b.9>

- American Public Health Association (APHA). 1998 Standard Methods for the Examination of Water and Wastewater, 20th edn. American Public Health Association/American Water Works Association/Water Environment Federation, Washington, DC, USA. APHA-Standard Methods of Water and Wastewater. 21st Edn., American Public Health Association, Washington, DC., ISBN: 0875530478 (2005) pp: 2-61
- APHA, 2005. Standard Methods of Water and Wastewater. 21st Edn., American Public Health Association, Washington, DC., ISBN: 0875530478, pp: 2-61
- Aruf, M., Muhammad, A., Sulaiman, M., Usman, H. M., Panda, S. L., & Idris, I. M. (2024). Water quality assessment and health implications: A study of Kano metropolis, Nigeria. *Journal of Science and Technology*, 9(6), 33-52. DOI : [10.46243/jst.2024.v9.i6.pp33-52](https://doi.org/10.46243/jst.2024.v9.i6.pp33-52)
- Bashir, M. Z. (2018). Geology of The Area Around Kurafe Hausawa, Part of Keffi Sheet 208 nw. 61.
- Dada, S. S. "Proterozoic evolution of Nigeria. (2006). " *The basement complex of Nigeria and its mineral resources (A Tribute to Prof. MAO Rahaman)*. Akin Jinad and Co. Ibadan 29-44. DOI: <https://doi.org/10.1016/j.emcon.2023.100207>
- Durov, S. A. (1948). Natural waters and graphical representation of their composition: *Doklady Akademii Nauk. Union of Sovietic Socialist Republics*, 59, 87-90.
- Egbueri, J. C., & Unigwe, C. O. (2020). Understanding the extent of heavy metal pollution in drinking water supplies from Umunya, Nigeria: an indexical and statistical assessment. *Analytical letters*, 53(13), 2122-2144.
- Emenike, C., Omo-Okoro, P., Pariatamby, A., Barasarathi, J., & Hamid, F. S. (2024). Remediation of Leachate-Metal-Contaminated Soil Using Selected Bacterial Consortia. *Soil Systems*, 8(1), 33. <https://doi.org/10.3390/soilsystems8010033>
- Fu, X., Chen, X., Xie, F., Zhang, Z., Ma, T., Dong, X., & Zheng, L. (2024). Combining APCS-MLR model to evaluate the distribution and sources of Rare Earth Elements in a large catchment. *Environmental Pollution*, 125256.
- Gyabaah, D., Awuah, E., Kuffour, R. A., Antwi-Agyei, P., Wiafe, S., & Asiedu, S. B. (2024). Assessment of dumpsites leachate, geotechnical properties of the soil, and their impacts on surface and groundwater quality of Sunyani, Ghana. *Environmental Advances*, 16, 100548.
- Jiriko, G. K., Dung Gwom Jy, and S. D. Wapwera. 2015. "The Evolution of Abuja as A 'Smart City' a Prognosis."
- Machado, D. V., Marques, E. D., Viglio, E. P., dos Santos, E. A. M., Amarante, R. T., da Silva Júnior, G. C., & Silva-Filho, E. V. (2024). High-resolution mapping and multivariate technique (factor analysis) to support hydrogeochemical analysis and identification of surface water contamination. *Journal of Geochemical Exploration*, 263, 107495.
- Melad, R. S., Nonato, R. L. V., Salazar, D. J., Ligaray, M. V., & Choi, A. E. S. (2024). Spatial assessment of water quality in Mananga River in Talisay City, Cebu, Philippines. *Results in Engineering*, 24, 103030. DOI: <https://doi.org/10.1016/j.rineng.2024.103030/>
- NASRDA - Department of Strategic Space Application, National Space Research and Development Agency, (2018). Benefits of Nigeria Satellite.

- Nayak, J., Singh, R., & Ganguly, R. (2024). Assessment of water quality in terms of the water quality index. In *Integrated Management of Water Resources in India: A Computational Approach: Optimizing for Sustainability and Planning* (pp. 105-120). Cham: Springer Nature Switzerland. DOI: https://doi.org/10.1007/978-3-031-62079-9_6
- NGSA (Nigeria Geological Survey Agency) (2011). Geological map of Abuja Published by the Authority of the Federal Republic of Nigeria
- NPCN (2016). Bureau of Statistic. Data from Nigerian Population Commission of Nigeria.
- NSDQW (2007). Nigerian Standard for Drinking Water Quality, Nigerian Industrial Standard NIS 554, Standard Organization of Nigeria, pp. 30.
- Obute, C. F., Ofon, U. A., Dunkwu-Okafor, A., Ndubuisi-Nnaji, U. U., & Amaowoh, U. G. (2024). Dynamics in Physicochemical and Bacteriological Properties of Simulated Leachate from Dump Site Soil in Ikhueni, Benin City, Edo State, Nigeria. *UMYU Journal of Microbiology Research (UJMR)*, 9(2), 66-74. DOI: <https://doi.org/10.47430/ujmr.2492.007>
- Ocheoibo, S. J., & Atuanya, E. I. (2024). Evaluation of Microbial Load and Physicochemical Characteristics of Soils in Electronic Waste Dumpsites of Oluku and Osasogie in Benin, Edo State and Alaba in Lagos State, Nigeria. *Journal of Applied Sciences and Environmental Management*, 28(3), 953-960. DOI: [10.4314/jasem.v28i3.37](https://doi.org/10.4314/jasem.v28i3.37)
- Piper, A. M. (1944). A graphic procedure in the geochemical interpretation of water analyses. *Eos, Transactions American Geophysical Union*, 25(6), 914-928.
- Raimi, M., Sawyerr, H., Ezekwe, C., and Salako, G. (2022). Many oil wells, one evil: Comprehensive assessment of toxic metals concentration, seasonal variation and human health risk in drinking water quality in areas surrounding crude oil exploration facilities in rivers state, Nigeria. 6, 23–42. DOI: <https://doi.org/10.15406/ijh.2022.06.00299>
- Sghiouer, F. E., Nahli, A., Bouka, H., & Chlaida, M. (2024). Analysis of the drought effects on the physicochemical and bacteriological quality of the Inaouene River water (Taza, Morocco). *Scientific African*, 25, e02328. DOI: <https://doi.org/10.1016/j.sciaf.2024.e02328>
- Singh, P. K., Kumar, U., Kumar, I., Dwivedi, A., Singh, P., Mishra, S., ... & Sharma, R. K. (2024). Critical review on toxic contaminants in surface water ecosystem: sources, monitoring, and its impact on human health. *Environmental Science and Pollution Research*, 1-35.
- SON (2015). Nigerian Standard for Drinking water Quality NIS 554: 2007 Standard Organization of Nigeria, Technical Report.
- Ukah, B. U., Egbueri, J. C., Unigwe, C. O., and Ubido, O. E. (2019). Extent of heavy metals pollution and health risk assessment of groundwater in a densely populated industrial area, Lagos, Nigeria. *International Journal of Energy and Water Resources*, 3, 291-303.
- WHO (2011) Edition, F. (2011). Guidelines for drinking-water quality. Geneva. *WHO chronicle*, 38(4), 104-8.

WHO (2017). World Health Organisation, Guidelines for Drinking-Water Quality. 4th Edition, World Health Organization, Geneva

World Health Organization (WHO) (2004) Guidelines for drinking water quality: incorporating 1st and 2nd Addlenda, vol 1. World Health Organization, Geneva

World Health Organization. (2008). *Guidelines for drinking-water quality: second addendum. Vol. 1, Recommendations*. World Health Organization.